The *Overgrown Hematopoietic Organs-31* Tumor Suppressor Gene of *Drosophila* Encodes an *Importin*-like Protein Accumulating in the Nucleus at the Onset of Mitosis

Istvan Török,* Dennis Strand,* Rolf Schmitt,* Gabriella Tick,‡ Tibor Török,‡ Istvan Kiss,‡ and Bernard M. Mechler*

*Department of Development Genetics, Deutsches Krebsforschungszentrum, Im Neuenheimer Feld 280, D-69120, Germany; and ‡Institute of Genetics, Biological Research Center of the Hungarian Academy of Sciences, Temesvàri krt 62, H-Szeged 6701, Hungary

Abstract. The tumor suppressor gene *overgrown hematopoietic organs- 31* (*oho31*) of *Drosophila* encodes a protein with extensive homology to the *Importin* protein of *Xenopus* (50% identity), the related yeast *SRP1* protein, and the mammalian *hSRP1* and *RCH1* proteins. A strong reduction in the expression of *oho31* by a P element inserted in the 5′ untranslated region of the *oho31* transcript or a complete inactivation of *oho31* by imprecise P element excision leads to malignant development of the hematopoietic organs and the genital disc, as shown by their growth autonomy in transplantation assays. We have cloned the *oho31* gene of *Drosophila melanogaster* and determined its nucleotide sequence. The gene encodes a phosphoprotein of 522 amino acids made of three domains: a central hydrophobic domain of eight repeats of 42–44 amino acids each, displaying similarity to the *arm* motif found in junctional and nucleopore complex proteins, and flanked by two hydrophilic NH_2- and COOH-terminal domains. Immunostaining revealed that the *OHO31* protein is supplied maternally and rapidly degraded during the first 13 nuclear divisions. Thereafter, the *OHO31* protein is predominantly expressed, albeit at reduced levels, in proliferating tissues. During the interphase of early embryonic cell cycles, the *OHO31* protein is present in the cytoplasm and massively accumulates in the nucleus at the onset of mitosis in late interphase and prophase. The nuclear import of *OHO31* is, however, less pronounced during later developmental stages. These results suggest that, similar to *Importin*, *OHO31* may act as a cytosolic factor in nuclear transport. Moreover, the cell cycle–dependent accumulation of *OHO31* in the nucleus indicates that this protein may be required for critical nuclear reactions occurring at the onset of mitosis.

THE potential to genetically dissect tumorigenesis constitutes one of the major reasons to study this process in *Drosophila*. Genetic analysis of this organism has led to the identification of >50 genes in which homozygous mutations cause tumors in tissues such as the imaginal discs, the brain, the hematopoietic organs, or the germ line (Gateff and Schneiderman, 1969, 1974; Gateff, 1978; Gateff and Mechler, 1989; Mechler, 1990; Mechler and Strand, 1990; Török et al., 1993*b*; Watson and Bryant, 1993; Mechler, 1994). Anatomical and histological examination of the mutant larvae have shown that the pattern of growth abnormalities is locus specific, with tumor formation taking place recurrently in the same organs. With the exception of tumors in the germ line, which cause sterility but no other deleterious effect, tumors occurring in other organs give rise to massive tissue overgrowth during larval development and lead to the death of the animals as late larvae or pupae. In *Drosophila*, most of the mutations affecting genes controlling tissue overgrowth are selected by their recessive lethal effect. Since the normal allele is dominant over the mutant allele, these genes are designated as tumor suppressor genes.

Molecular investigations of several tumor suppressor genes in *Drosophila* have shown that tumorigenesis may result from the disruption of distinct regulatory pathways. Based on the presumed function of the encoded protein, which in many cases has been inferred by virtue of sequence similarities with proteins of known function, the *Drosophila* tumor suppressor genes fall into five categories (Watson and Bryant, 1993; Mechler, 1994). These genes encode (*a*) cell surface proteins, which may control cell adhesion (Mahoney et al., 1991); (*b*) junctional proteins, which may mediate signal transduction (Woods and

Address all correspondence to B. M. Mechler, Department of Developmental Genetics, DKFZ, Im Neuenheimer Feld 280, D-69120 Heidelberg, Germany. Tel.: (49) 6221 42 45 02. Fax: (49) 6221 42 45 52.

Bryant, 1991, 1993; Boedigheimer and Laughon, 1993); (*c*) cytoskeletal proteins, which may play a direct role in the cell architecture and may, in addition, mediate a signaling pathway in the cytoplasm (Mechler et al., 1985; Jacob et al., 1987; Strand et al., 1994*a*,*b*); (*d*) cytoplasmic proteins involved in vesicular trafficking and, thus, regulating intercellular transfer of signals (Chen et al., 1991; Van der Bliek and Meyerowitz, 1991); and (*e*) ribosomal proteins, which may act as regulators of translation (Watson et al., 1992; Stewart and Denell, 1993).

In *Drosophila*, mutations in >25 genes can cause overgrowth of hematopoietic organs during larval development (Gateff and Mechler, 1989; Watson et al., 1991; Török et al., 1993*b*). Hematopoietic organs are formed by five to seven pairs of glandular structures (the lymph glands) located along the dorsal heart vessel behind the brain hemispheres and produce hemocytes by a stem cell mechanism. In wild-type larvae, the hemocytes are released into the hemolymph at the end of the third larval instar (Rizki, 1978; Shrestha and Gateff, 1982). In mutants, the growth and differentiation of these cells are disrupted, giving rise to overgrowth of the hematopoietic organs. This overgrowth can be accompanied by a premature release of hemocytes into the hemolymph. In turn, the circulating hemocytes can proliferate in the hemocoele, either invading the entire body cavity and destroying all other organs or forming secondary masses, which may ultimately become melanized. One example of the latter category is the mutation *lethal(2)144/1*, which was recovered in a genetic screen designed for identifying genes located on the second chromosome of *Drosophila melanogaster* controlling cell proliferation and tumorigenesis (Török et al., 1993*b*). On the basis of its mutant phenotype, the gene was renamed *overgrown hematopoietic organs-31* (*oho31*).

In this study, we have cloned and sequenced the *oho31* gene of *D. melanogaster*. We found that the predicted protein sequence is remarkably similar to the sequence of four recently identified proteins forming a growing family of structurally related proteins, namely: (*a*) the *Importin* protein of *Xenopus*, which has been identified as a cytosolic factor involved in nuclear protein import (Görlich et al., 1994); (*b*) the yeast *SRP1* protein, a suppressor of temperature-sensitive RNA polymerase I mutations (Yano et al., 1992), which was found to interact directly with two nuclear pore proteins NUP1 and NUP2 (Belander et al., 1994); (*c*) the mammalian *SRP1* proteins (Cortes et al., 1994); and (*d*) the mammalian *RCH1* proteins (Cuomo et al., 1994). Both mammalian proteins were identified through their interaction with the *RAG-1* recombination-activating protein in a yeast two-hybrid assay. These proteins as well as the *OHO31* protein contain a central region made of eight degenerate 42–amino acid repeats. This reiterated motif, known as the *arm* motif, was first identified in the *Drosophila* segment polarity gene *armadillo* (Riggleman et al., 1989) and recently found in several proteins with diverse cellular functions (Peifer et al., 1994). Analysis of the spatio-temporal expression of *OHO31* during *Drosophila* development showed that the protein is essentially expressed in dividing tissues and displays a dynamic intracellular distribution. During the entire cell cycle, the *OHO31* protein is predominantly present in the cytoplasm with the exception of prophase when it becomes associated with nuclei. This is the first example of a tumor suppressor gene involved in nuclear protein import.

Materials and Methods

Drosophila Strains, Culture Conditions, and Analysis of the Larval Lethal Phenotype

The *y w; oho31$^{144/1}$/CyO P(y$^+$)* flies contain a *CyO P[y$^+$]* balancer chromosome carrying a *P(y$^+$)* insertion, which was kindly provided by Allen Shearn (The Johns Hopkins University, Baltimore, MD). The *y$^+$* marker is particularly useful for selecting homozygous *oho31$^{144/1}$* larvae. The fly cultures were reared at 25°C on standard cornmeal–yeast–agar medium with or without addition of molasses–soya flour–malt extract. Since the lethal tumorous phenotype of the *oho31* larvae was the same on both media, no distinction was made in the text in this respect. *oho31* homozygous larvae survive for a long period of time as late third instar larvae and die without puparium formation (Török et al., 1993*b*). As the overgrowth phenotype develops gradually during the prolonged survival period, *y oho31*–mutant larvae were selected and kept on fresh medium in a humidified atmosphere. The overgrowth phenotype of the different organs was examined by dissecting the aged larvae, usually 15–20 d after egg laying, in Ringer's (Becker, 1959) under a stereomicroscope. For the examination of cell nuclei, dissected tissues were fixed in 0.5% glutaraldehyde for 30 min, and then stained for 15–20 min with 2.5 μg/ml HOECHST 33258 (Sigma Chemical Co., St. Louis, MO) dissolved in Ringer's. The stained tissues were examined under a Leitz fluorescence microscope (Leica Vertrieb GmbH, Bensheim, Germany).

Isolation of Deletions by Imprecise Excision of the P Element

The *PlacW* insert at position 31A was remobilized by crossing *y w/Y; oho31$^{144/1}$/CyO P[y$^+$]* males to *y w; Δ2-3 Sb/TM6 Ubx* females. In the F_0 generation, *y w/ Y; oho31/$^+$; Δ2-3 Sb/+* "jumpstarter" males were collected and crossed with *y w; Sco/CyO P[y$^+$]* females. In the F_1 generation, *y w/Y; oho31$^{Df(?)}$/CyO P[y$^+$]* males were crossed with *y w; Sco/CyO P[y$^+$]* females. From the F_2 generation, stocks were established by crossing *y w; oho31$^{Df(?)}$/CyO P[y$^+$]* males and females together. Lines that did not produce *y Cy$^+$* flies in the subsequent generation were likely carriers of deficiencies in *oho31*.

Transplantation of Tumorous Tissues

Tumorous larvae were surface sterilized with 70% ethanol for 10 min and dissected in sterile Ringer's. The tumorous tissues were cut into ~10–20-μm fragments and injected into the abdominal cavity of young egg-laying females by using glass needles ~20 μm in diameter. The host flies were kept on fresh medium, which was changed every 3–4 d when the flies were examined. Hosts carrying a successfully growing implant were recognized by their bloated abdomen. The flies were dissected and the implants examined under a compound microscope.

Nucleic Acid Procedures

Unless otherwise indicated, DNA isolation, cloning, and analysis were performed according to standard protocols (Sambrook et al., 1989). Genomic DNA fragments from both sides of the P element insertion were recovered by plasmid rescue. DNA from heterozygous *oho31$^{144/1}$ CyO* flies was digested with EcoRI or BamHI, ligated, and transformed into XL-1 blue–competent cells. The rescued clones were analyzed by restriction digestion and Southern hybridization with pUC18 and P element inverted repeat specific probe. Genomic fragments without a P element sequence were then used to screen a genomic library in EMBLA-λ phages. Two probes, as defined in Fig. 2 *c* (probes A and B), were used to screen two cDNA libraries made with polyA$^+$RNa extracted from 0–9-h-old embryos in λZapII (Stratagene Corp., La Jolla, CA), made by I. Török, or 0–16-h-old embryos in λgt11, kindly provided by L. Kauvar (Poole et al., 1985). The inserts of the λ gt11 phages were subcloned into Bluescript SK$^+$ vector, and the inserts from λZAPII phages were recovered by in vivo excision. cDNA inserts and genomic clones were sequenced by using the ExoIII deletion procedure (Henikoff, 1984). Sequencing was carried out with double- or single-stranded DNA templates and conventional T3, T7, and universal primers. The insertion site of the P element in the genomic sequence was

determined by sequencing the rescued plasmids with an oligonucleotide (18-mer) primer located inside the inverted repeat of the P element at 10 nucleotides from its extremity. PolyA$^+$RNA was isolated, electrophoresed, and transferred to nitrocellulose filters (Schleicher & Schuell GmbH, Dassel, Germany), or Hybond-N filters (Amersham, Buckinghamshire, UK), as described in Török et al. (1993*a*). Probes were either generated by random priming or made of specific antisense single-stranded DNA synthesized by asymmetric PCR using T3 or T7 primers and [^{32}P]α-dCTP, according to the procedure of Patel and Goodman (1992).

Whole-Mount in situ Hybridization

Developmentally staged embryos were prepared and fixed as described in Tautz and Pfeifle (1989). Brain and discs from wild-type Oregon R or *oho31$^{144/1}$* homozygous mutant third instar larvae were dissected in PBS and fixed in 4% formaldehyde in PBS at room temperature for 20 min. Hybridization and staining procedures were made according to Tautz and Pfeifle (1989). Digoxygenin-labeled RNA probes were synthesized in vitro by using subclones from the 3′ or 5′ noncoding ends of the cDNAs in Bluescript SK$^+$ vector and T3 or T7 RNA polymerases. Before hybridization, the RNA probe was reduced in size by mild alkaline hydrolysis. Digoxygenin-labeled single-stranded DNA probes were made by asymmetric PCR synthesis according to Patel and Goodman (1992).

In Vitro Translation

In vitro translation was performed by using the TNT transcription–translation–coupled reticulocyte lysate system (Promega Biotec, Madison, WI) and the cDNAs subcloned in pBluescript SK$^+$ vector (Stratagene Corp.).

Preparation of OHO31 Antibodies

Antibodies directed against the *OHO31* protein were prepared using two distinct hybrid proteins as immunogens. The first fusion protein contains 301 residues from the central domain (amino acid positions 123–423) of *OHO31* fused to a his-tag peptide in a pET-15b expression vector (Novagen, Madison, WI). The second fusion protein contains the COOH-terminal 244 residues (amino acid positions 279–522) of *OHO31* fused to glutathion S-transferase in a pGEX-2T expression vector (Pharmacia Inc., Piscataway, NJ). The hybrid protein expressed from plasmid pET-15b was induced with 1 mM isopropyl-β-D-thiogalactoside (IPTG) in BL-21 (DE3) *Escherichia coli* bacteria and purified to near homogeneity on a His.Bind resin column (Novagen). The hybrid protein expressed from plasmid pGEX-2T was similarly induced with IPTG and purified on a glutathion–Sepharose 4B column as indicated in the instructions provided by the manufacturer (Pharmacia Inc.). The purified hybrid proteins were used to immunize rabbits. Polyclonal antibodies were purified by a two-step affinity chromatography procedure, using first a protein A–agarose colum (Boehringer Mannheim GmbH, Mannheim, Germany) and then either a *OHO31$^{his\text{-}tag}$* or a *OHO31$^{glutathion\ tranferase}$* Sepharose 4B column. Finally, the affinity-purified anti-*OHO31* antibodies were preadsorbed on proteins extracted from homozygous *oho31^{D14}* lethal larvae deficient for the major part of the *oho31* coding sequence.

Immunohistochemistry

Embryos were dechorionated in 3% bleach (Roth GmbH, Karlsruhe, Germany) and washed extensively in 0.1% Triton X-100 and deionized H_2O. Fixation was performed by shaking the embryos in 4% formaldehyde in PEM buffer (100 mM Pipes [pH 6.9], 2 mM EGTA, 1 mM $MgSO_4$) with an equal volume of heptane. The embryos were devitellinized by vigorous shaking in 1:1 heptane/methanol and rehydrated in PBS containing 0.1% Triton X-100 (PBT)[1]. Brain–disc complexes were dissected in PBS, fixed in 4% formaldehyde in PBS for 20 min at room temperature, and extensively washed in PBT. The brain–disc complexes were then blocked overnight in PBT containing 5% normal goat serum and 1% BSA. Anti-*OHO31* antibodies were diluted 1:50 in the blocking solution and incubated with the embryos or the dissected tissues overnight at 4°C in a humidified chamber. After three washes in PBT, the embryos and the tissues were incubated for 2 h at room temperature with biotinylated goat anti–rabbit antibodies. HRP staining was performed with the Vectastain Elite ABC Kit (Vector Laboratories, Inc., Burlingame, CA) according to the manufacturer's instructions. After three washes with PBS, the embryos and tissues were transferred on slides and mounted in Kaiser's glycerin gelatin (Merck GmbH, Darmstadt, Germany). For double fluorescence labeling experiments, the embryos were first incubated with anti-*OHO31* antibodies, as described above. Goat anti–rabbit antibodies conjugated with FITC (Jackson ImmunoResearch Laboratories, Inc., West Grove, PA) were first preadsorbed on fixed embryos in a 1:5 dilution in PBT at 4°C, and then applied to the anti-*OHO31*–labeled embryos as a mixture at a 1:400 dilution. DNA was stained after RNaseA treatment (400 μg/ml for 2 h in PBS) with 5 μg/ml propidium iodide for 30 min at room temperature and washed overnight at 4°C in PBS. The embryos were mounted in Vectashield embedding medium (Vector Laboratories, Inc.) and inspected under a Leitz fluorescence microscope, (Leica Vertrieb GmbH) or a confocal laser scanning Zeiss microscope (Carl Zeiss Jena GmbH, Jena, Germany).

Western Blot Analysis, Immunoprecipitation, and Phosphatase Treatment

Protein extracts from different stages of *Drosophila* development were prepared by homogenizing 1 g tissue in 4 ml cracking buffer (0.125 M Tris [pH 6.8], 5% β-mercaptoethanol, 2% SDS, 4 M urea) using a motor-driven homogenizer at 4°C. Aliquots containing equal amount of proteins were diluted 1:1 in 2× Laemmli sample buffer and boiled for 5 min. The proteins were separated on 7 or 10% SDS–polyacrylamide gels. After electrophoresis, proteins were electrotransferred to Immobilon-P polyvinylidenfluoride (PVDF) membranes (Millipore Corp., Bedford, MA) using a Multiphore semidry transfer apparatus (LKB Instruments, Inc., Bromma, Sweden). Secondary antibodies for Western blotting were coupled to alkaline phosphatase as provided in the Tropix system (Serva Feinbiochemica GmbH, Heidelberg, Germany) and used as recommended by the manufacturer. For immunoprecipitation analysis, the embryos were homogenized at 4°C in RIPA buffer (50 mM Tris, pH 8.5, 300 mM NaCl, 1% NP-40, 0.5% sodium deoxycholate, 0.1% SDS, and 2.5 mM EDTA) containing the following proteinase inhibitors: 1 μg/ml leupeptin, 1.4 μg/ml pepstatin, 0.1 mg/ml Tosyl-L-phenylalanin-chloromethylketon, 10 μg/ml soybean trypsin inhibitor, 5 μg/ml aprotinine, and 0.1 mg/ml PMSF. After clearing of the extracts at 13,000 *g* for 15 min at 4°C, the supernatants were incubated with 15 μg affinity-purified anti-*OHO31* polyclonal antibodies and 50 μl protein A–Sepharose (Boehringer Mannheim GmbH) for 2–4 h on rotating wheel at 4°C. The Sepharose beads were washed three times in RIPA buffer and either boiled in 2× Laemmli loading buffer or used for phosphatase treatment. Phosphatase treatment was performed as described by Suter and Steward (1991). The immunoprecipitates were further washed in RIPA/PAP (potato acid phosphatase) buffer (1:1) and then resuspended in PAP buffer (1 mM Pipes, pH 6.0, 150 mM NaCl). The immunoprecipitates were then incubated with either 0.5–1 U PAP in the same buffer or 5 U calf intestine alkaline phosphatase (CIAP) in 50 mM Tris (pH 8.5) and 300 mM NaCl for 20 min at 37°C. The reactions were stopped by adding an equivalent volume of 2× Laemmli loading buffer, boiled, and loaded onto 7 or 10% SDS–polyacrylamide gels. After gel electrophoresis, the proteins were transferred to Immobilon-P PVDF membranes and probed with anti-*OHO31* antibodies using the Tropix chemiluminescence system.

Results

Genetic Localization and Phenotype

The mutation *144/1* resulted from the insertion of a single *P-lacW(Pw$^+$-LacZ)* transposon (Bier et al., 1989) integrated within the chromosomal region 31A on the second chromosome (Török et al., 1993*b*). Homozygous mutant larvae showed a typical class II *air* lethal phenotype (Watson et al., 1991) with abnormal development of the hematopoietic organs (lymph glands), the occurrence of numerous masses of hemocytes dispersed all over the body cavity, and the formation of melanotic tumors (Fig. 1 *A*). Confirmation that the P element insertion was the cause of

1. *Abbreviations used in this paper*: AED, after egg deposition; CIAP, calf intestine alkaline phosphatase; ORF, open reading frame; PAP, potato acid phosphatase; PBT, PBS plus Triton X-100; PVDF, polyvinylidenfluoride.

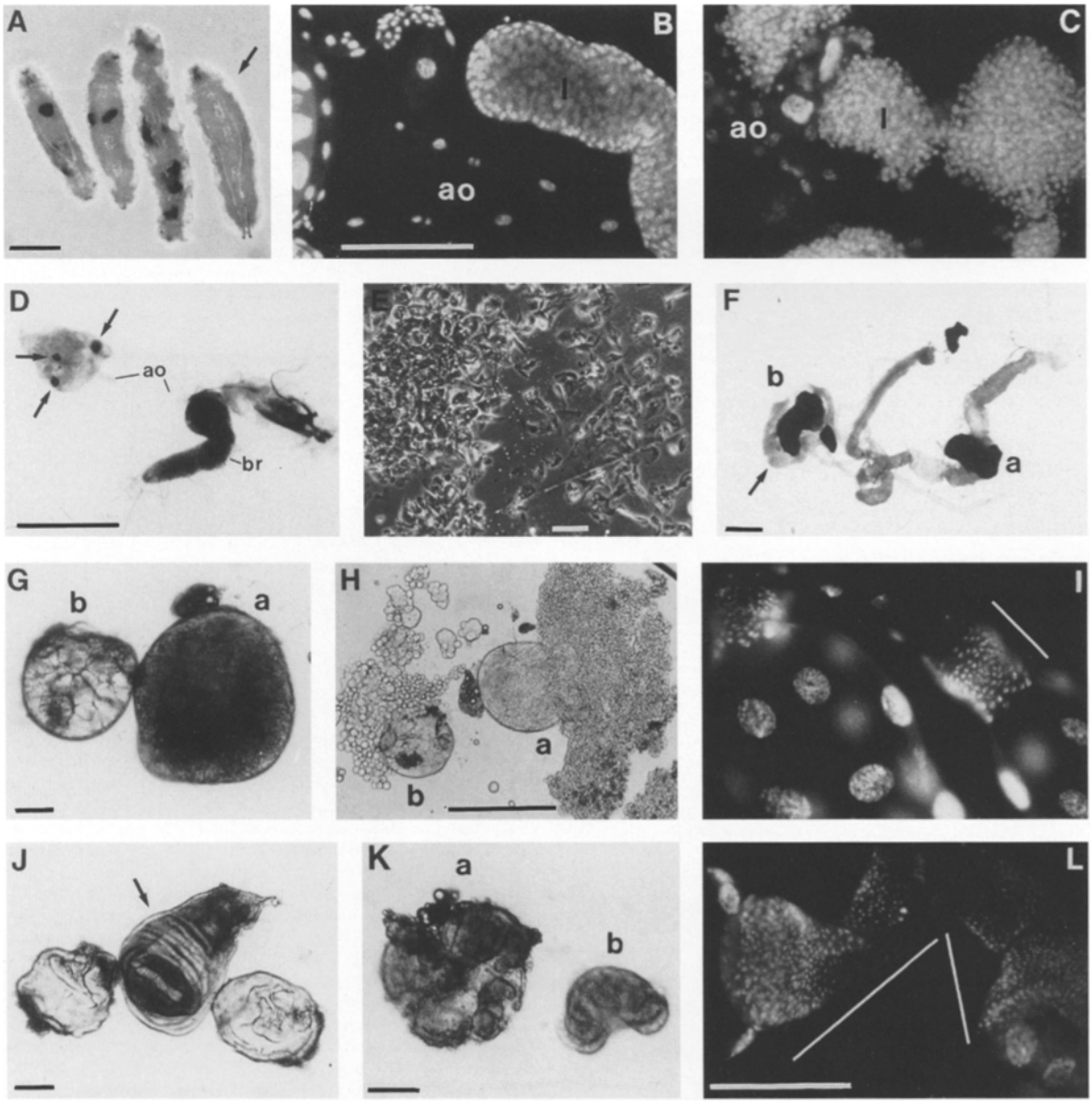

Figure 1. Morphology of wild-type and mutant *oho31* larvae and tissues. (*A*) Homozygous *oho31* and wild-type (*arrow*) larvae. Multiple melanized hemocytic tumors are apparent in the mutant larvae. Whole-mount lymph glands of wild-type (*B*) and *oho31* (*C*) larvae were stained with HOECHST 33258; position of the aorta (*ao*) and lymph glands (*l*) are indicated. The cells of *oho31* lymph glands are visibly more scattered than in wild-type lymph glands. (*D*) Brain and hypertrophied lymph glands of an older surviving *oho31* larva showing three initial foci of melanization (*arrows*). Positions of aorta (*ao*) and brain (*br*) are indicated. (*E*) Lamellocytes from a partially dissociated *oho31* hemocytic tumor. (*F*) Melanotic masses of hemocytes associated with the midgut (*a*) and the Malpighian tubules (*b*) of an *oho31* homozygous larva. In the tumor associated with the Malpighian tubules, the melanized core is surrounded by a nonmelanized layer of hemocytes (*arrow*). (*G*) *oho31* mutant (*a*) and wild- type (*b*) testes. Spermatogonial cysts are visible in *b*. (*H*) Partially disrupted *oho31* (*a*) and wild-type (*b*) testes, identical to those shown in *G*. Spermatogonial cysts of different sizes poured out of the wild-type testis, while the mutant testis contained single cells of uniform size. Imaginal rings in whole-mount salivary glands from wild-type (*I*) and *oho31* (*L*) mutant third instar larvae. The number of diploid nuclei of the imaginal rings and the areas (*solid lines*) they cover are obviously larger in the mutant. (*J*) Wing imaginal discs from *oho31* mutant and wild-type (*arrow*) late third instar larvae. The mutant discs display a reduced size and an abnormal folding pattern. (*K*) Female genital discs of *oho31* mutant (*a*) and (*b*) wild-type late third instar larvae. Bars: (*A*, *D*, and *H*) 500 μm; (*G*, *J*, and *K*) 100 μm; (*B*, *F*, and *L*) 50 μm; (*E*) 5 μm.

the mutant phenotype was obtained by reversion of the mutation to wild type after remobilization of the *P-lacW* transposon (Török et al., 1993*b*). On the basis of the overgrowth of the hematopoietic organs and the localization of the P element insert, we named the gene *overgrown hematopoietic organs-31* (*oho31*).

In wild-type third instar larvae, the hematopoietic organs consist typically of four to seven small paired lobes arranged along the dorsal aorta and made of tightly associated cells (Fig. 1 *B*). In *oho31* third instar larvae, the lymph glands at first look apparently normal, while in older surviving larvae, they increase considerably in size

forming loose masses of aggregated hemocytes associated with the aorta (Fig. 1, *C* and *D*) or almost completely disappearing with the formation of secondary nodules of hemocytes dispersed in the entire body cavity. As shown in Fig. 1 *C*, the cells in the lymph glands of young third instar mutant larvae appear to be loosely attached and tend to dissociate from each other upon manipulation, whereas in normal lymph glands (Fig. 1 *B*), the cells are more tightly bound to each other and form compact organs. In surviving mutant larvae, that is, older than 4 d, small nodules of aggregated hemocytes can be found in the body cavity, and their number and size increase with time. These amorphic masses are made of loosely attached hemocytes, which, upon dissection and manipulation, tend to dissociate into single elongated cells (Fig. 1 *E*). In aging larvae, some of these nodules increase in size, becoming more compact and punctated with small foci of melanization (Fig. 1 *D*), which eventually spread over the entire hemocytic mass (Fig. 1 *F*). Although the location of these melanotic tumors varies, we found them frequently around the digestive tube in the vicinity of the midgut–hindgut boundary and/or associated with the Malpighian tubules (Fig. 1 *F*).

In addition to abnormalities in the lymph glands, some other organs show overgrowth. The most frequently affected organs are the gonads, particularly the testes, which may increase two to two and half times in diameter (Fig. 1 *G*). By comparison to wild type, the mutant testes are devoid of spermatogonial cysts but filled up with small uniform single cells (Fig. 1 *H*). In very old mutant larvae, the size of the imaginal rings of the salivary glands is also consistently larger than normal (Fig. 1, *I* and *L*). Despite the large increase in cell number, the epithelial structure of this tissue is maintained.

In *oho-31* third instar larvae, most of the imaginal discs (wing, leg, haltere, eye/antenna) remain smaller than normal, with a fully distorted shape and abnormal folding pattern (Fig. 1 *K*), although these discs may occasionally become overgrown in very old larvae. By contrast, the genital disc is consistently much larger than normal (Fig. 1 J). The brain organization displays abnormalities, which are more pronounced in old mutant larvae. The hemispheres are smaller than normal, with an elongated shape, and the ventral ganglion is often longer than normal, (data not shown). No other gross abnormalities can be observed in the remaining organs. The polytenic larval tissues, including the ring gland, exhibit an apparently normal morphology, albeit with a somewhat reduced size. In conclusion, the *oho31* mutation exerts a pleiotropic effect on several presumptive adult tissues during the larval development, with the most dramatic effect being on the hematopoietic organs, the genital disc, the gonads, and the imaginal rings of the salivary glands.

A series of 20 nonviable w^- revertants were generated by imprecise excision of the P element after remobilization. Their molecular analysis showed that two of them had small deficiencies removing the presumptive *oho31* transcription unit (vide infra). Animals homozygous for the deficiencies, or transheterozygous animals combining the original *144/1* mutation with one of the deficiencies, display in all respects a phenotype similar to that of the *144/1* homozygotes. These results indicate that the original *144/1* mutation can be genetically considered as a null allele of the *oho31* gene, and the phenotype described above results from a complete or nearly complete absence of *oho31* function.

Transplantation of Mutant Tissues

Fragments of overgrown tissues from *oho31*$^{144/1}$ larvae were transplanted into the abdomen of wild-type female hosts to test for autonomous growth. Two types of tissues were tested: the hemocytic tumors present in the body cavity of *oho31* larvae and the overgrown genital discs. Transplanted fragments of these tissues gave rise to tumorous outgrowth in 4% (3/71) of the hemocytic tumors and in 13% (5/34) of the genital discs. Among the three successful hemocytic transplants, two produced nonmelanized hemocytic masses similar to the starting larval tumorous material, whereas the third transplant gave rise to a large tumor, which subsequently became fully melanized. The five genital disc fragments, which were able to grow in the host, formed amorphic masses of folded epithelium. Hosts carrying a successfully growing implant were recognized by the bloating of their abdomen. After dissection, we observed that the abdominal cavity was essentially filled by the growing implants, and the host ovaries were considerably atrophied. Implanted fragments of other tissues, such as the imaginal rings of the salivary glands or the imaginal wing discs, did not give rise to any visible growth in the

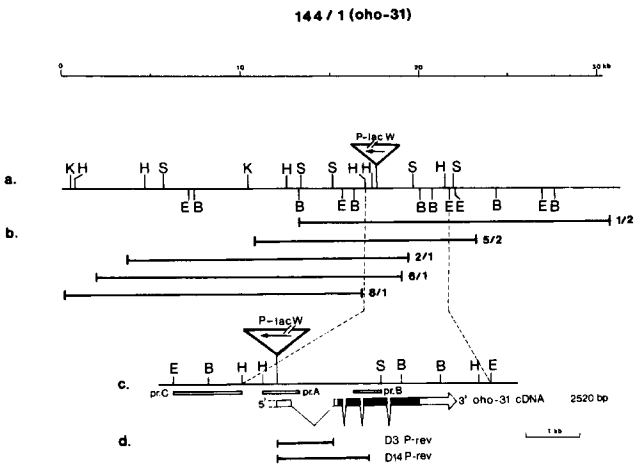

Figure 2. Map of the *oho31* region at 31A in *D. melanogaster*. (*a*) A composite map of ~30 kb of DNA from the *oho31* region is shown with the coordinate scale above the map. Coordinate 0 is chosen arbitrarily and lies at the left end of the cloned *Drosophila* DNA segment. The exact location of the *P-lacW* insertion was mapped by DNA sequencing, as indicated in Fig. 3. (*b*) Overlapping array of *Drosophila* inserts found in recombinant phages isolated from an Oregon R EMBL4-λ library. (*c*) Enlargement of the map around the site of the *P-lacW* insertion with localization of the genomic fragments pr.A, pr.B, and pr.C used for transcriptional mapping of the *oho31* locus. Below the map is depicted the exon organization of the *oho31* transcript as determined from sequence analysis of five cDNAs (see Fig. 3). The coding sequences are indicated by solid boxes and the noncoding transcribed regions by open boxes. (*d*) Interstitial deletions *D3* and *D14* within the *oho31* gene that have been induced by imprecise excision of the *P-lacW* element. Restriction sites: BamH1 (*B*); EcoRI (*E*); HindIII (*H*); Kpn1 (*K*); Sal1 (*S*).

host abdomen. These results show that not all the implanted fragments were able to grow, and indicate that only certain cells or regions of the dissected tumors have retained a potential for autonomous growth.

Isolation of Genomic and cDNA Clones

DNA flanking both sides of the *P-lacW* element located at position 31A were cloned by plasmid rescue. The recovered genomic DNA fragments were used to obtain λ phage clones from a wild-type genomic library. These clones were found to cover a chromosomal segment of ~35 kb around the P insertion site (Fig. 2). A transcript map for a region flanking ~10 kb on each side of the P element insertion site was generated by using subfragments of the λ phage clones. Probes A and B located on one side of the P element hybridized to a 2.8-kb polyA$^+$RNA present in early embryos, pupae, and adult flies as shown in Fig. 3, whereas probe C located on the other side of the insert recognized several polyA$^+$RNAs ~2, 4, and 7 kb in size and present in late embryos, larvae, and pupae (data not shown).

The assumption that *oho31* encodes the 2.8-kb RNA is based on three lines of evidence. First, Southern blot analysis revealed that 2 of the 16 lethal w^- revertants obtained by

Figure 3. Sequence of the *oho31* gene and predicted amino acid sequence of its product. Introns and untranscribed sequences are shown in lowercase letters; exons are shown in uppercase letters. The first nucleotides of the cDNAs *K1*, *K2*, *K4*, *K7*, and *K9* are indicated by an asterisk (*) and the last nucleotides of these cDNAs by an open circle (○) above the nucleotide sequence. The putative polyadenylation signal AATAAA is indicated by underlining, and the *nanos* responsive element GTTGT(Xn)ATTGTA is boxed. The GenBank/EMBL/DDBJ accession number for the genomic and amino acid sequences of *Drosophila oho31* is X85752.

P element remobilization resulted in the complete elimination of the P element with intragenic deletions removing DNA segments of 1.0 and 1.7 kb in the case of *D3* and *D14*, respectively. As shown in Fig. 2, one breakpoint of these two deletions lies at the site of P element insertion and the other within the 2.8-kb transcript. Third, the spatial and temporal expression of the 2.8-kb transcript in late third instar larvae was similar to the β-galactosidase expression originating from the inserted P element (data not shown).

Sequence Analysis and P Element Insertion Site

The nearly full-length sequence of the *oho31* mRNA was obtained from the cDNA *K2*. In addition, we have isolated and sequenced a total of five cDNAs whose sequences perfectly overlap with portions of *K2*. The nucleotide and deduced amino acid sequences of this cDNA (2,544 nucleotides in length) and the alignment of its nucleotide sequence on the genomic sequence are shown in Fig. 3. To determine the exact site of the insertion of the P element, we sequenced the genomic DNA flanking the P element flanking in clones isolated from the $oho31^{144/1}$ allele using a DNA primer derived from the sequence of the *P-lacW* inverted terminal repeat. On the wild-type genomic sequence, the *P-lacW* element is inserted 5 bp downstream from the 5′ end of the *oho31* cDNA *K2* (Fig. 3).

Comparison of the cDNA and genomic sequences revealed five exons separated by four introns of 415, 61, 63, and 64 nucleotides, respectively. The sequence contains an open reading frame (ORF) of 522 codons initiated by an ATG. This ORF encodes a protein with a predicted molecular mass of 58 kD. The first ATG in the long ORF is directly preceded by a polypurine track varying in length between 15 A in Oregon R genomic DNA and 23 A in cDNA *K2*. This polypurine track ends a 332-nucleotide AT-rich leader sequence without any ATG-initiated ORF. Although such a long A track preceding an ORF is quite unusual, it conforms to the *Drosophila* translation start consensus sequence ANN (C/A) A (A/C) (A/C) ATGN (Cavener, 1987). The long ORF is followed by an 630-nucleotide AT-rich 3′ untranslated sequence containing a canonical poly(A) addition site AATAAA located 23 nucleotides from the start of the poly(A) tract. This sequence is itself inserted into a motif resembling the *nanos* responsive element GTTGT(Xn)ATTGTA, which mediates the repression of translation of *hunchback* and *bicoid* RNA in response to the *nanos* gene product (Wharton and Struhl, 1991) or regulates cyclin B expression (Dalby and Glover, 1992).

oho31 Gene Is Intensively Expressed during Early Embryogenesis and More Moderately during the Larval to Pupal Transition Phase

To determine the expression and abundance of the *oho31* transcript during development, we performed Northern blot analysis of polyA$^+$RNA extracted from different developmental stages. As shown in Fig. 4, a single 2.8-kb polyA$^+$RNA species could be detected. The *oho31* message is abundant in preblastoderm embryos (0–2-h old embryos), and its concentration progressively decreases during blastoderm formation and gastrulation (0–3 and 3–6 h, respectively). During germ band extension (6–9 h), the *oho31* message is again expressed before disappearing almost completely in late embryonic stages. *oho31* expression resumes in late third instar larvae and becomes intense in early pupae. The *oho31* message is also present in adults; it is more abundant in females than in males, indicating that this message may be intensively produced in ovaries.

To investigate the spatio-temporal pattern of *oho31* RNA expression in *Drosphila* during embryonic development, we performed in situ hybridization of whole-mount embryos using digoxigenin-labeled single-stranded antisense RNA and DNA probes prepared from the cDNA *K2*. As shown in Fig. 5, *oho31* expression shows dramatic changes during embryonic development. At the earliest stage (0–2 h), when the embryos are undergoing rapid nuclear divisions in a syncytium, maternally derived *oho31* mRNA is present at a high concentration and is homogeneously distributed in the embryos (Fig. 5 *A*). Between cycles 10 and 13, the level of the *oho31* message decreases considerably in the cortical cytoplasm but remains relatively high in the pole cells (Fig. 5, *B–D*). Interestingly, this decrease is not homogenous but gives rise to a pattern of seven weak stripes along the anterior–posterior axis of the embryo (Fig. 5 *D*). At the beginning of gastrulation (Fig. 5 *E*), these stripes become more intense with the first stripe located anterior to the cephalic furrow. During germ band extension (Fig. 5 *F*), the *oho31* transcripts are essentially limited to the neuroblasts and the ventral ectoderm, where they are distributed in diffuse stripes. Beyond this stage (Fig. 5, *G* and *H*), *oho31* expression becomes limited to cells of the ventral nerve cord and to the proliferative centers of the brain lobes, where it shows a decreasing expression until late into embryonic development.

In situ hybridization of whole-mount tissues prepared from late third instar larvae reveals a high level of *oho31* RNA expression in all imaginal discs (Fig. 6 *A*) and a more moderate expression in the ring gland and the hematopoi-

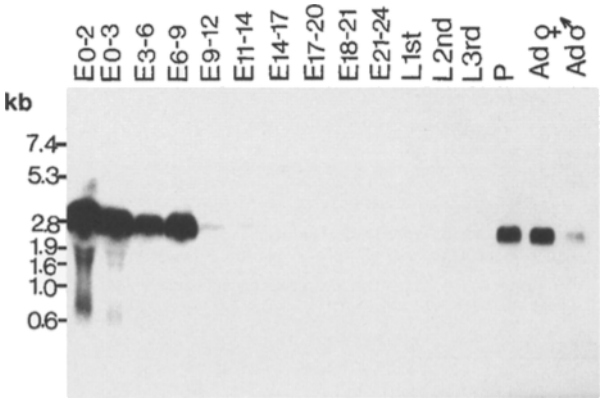

Figure 4. Abundance of *oho31* transcripts during development. This panel shows a developmental Northern blot probed with antisense single-stranded *K2* cDNA. Sequential hybridization with antisense single-stranded pr.A and pr.B DNA probes (see Fig. 2) gave the same hybridization pattern. PolyA$^+$RNA was quantified by hybridization with a β-tubulin probe so that equal amounts of polyA$^+$RNA were present in each fraction. Embryonic stages (0–2, 0–3, 3–6, 6–9, 9–12, 11–14, 14–17, 17–20, 18–21, and 21–24 h) are designated by E, larval stages (1st, 2nd and 3rd) are designated by L, pupal stage by P and adult females and males by Ad♂ and Ad♀, respectively.

etic organs associated with the aorta (Fig. 6 *B*). A low level of *oho31* expression can be detected in the brain hemispheres and the ventral ganglion. Examination of homozygous *oho31*$^{141\text{-}1}$ late third instar larvae reveals a similar pattern of β-galactosidase expression in imaginal discs, ring gland, and hematopoietic organs and a low expression in the brain (data not shown), indicating that the *oho31* promoter drives the expression of the *lacZ* gene present in the *p-lacW* element inserted in 31A.

oho31 Encodes a Protein with Extensive Homology to the Importin Protein of Xenopus, the Related Yeast SRP1 Protein, and the Mammalian SRP1 and RCH1 Proteins

The *OHO31* protein shares extensive similarity with a family of proteins identified in yeast as well as in vertebrates characterized by a central domain of eight degenerate 42–amino acid tandem repeats with no interruptions. As shown in Table I, *OHO31* is most similar to the *Xenopus Importin* (Görlich et al., 1994) and the mammalian *RCH1* proteins (Cuomo et al., 1994), and also displays similarity with the yeast *SRP1* protein (Yano et al., 1992, 1994) and the mammalian *SRP1* proteins (Cortes et al., 1994). As shown in Fig. 7, the sequence similarity is most pronounced in the region of the eight tandem repeats. The total length of the repeats accounts for approximately two thirds of the size of these molecules. In *OHO31*, the first, third, and last repeats (43, 43, and 44 amino acids, respectively) differ from the consensus length of 42 amino acids. The repeating motif is characterized by the presence of strongly preferred amino acids at many positions, as indi-

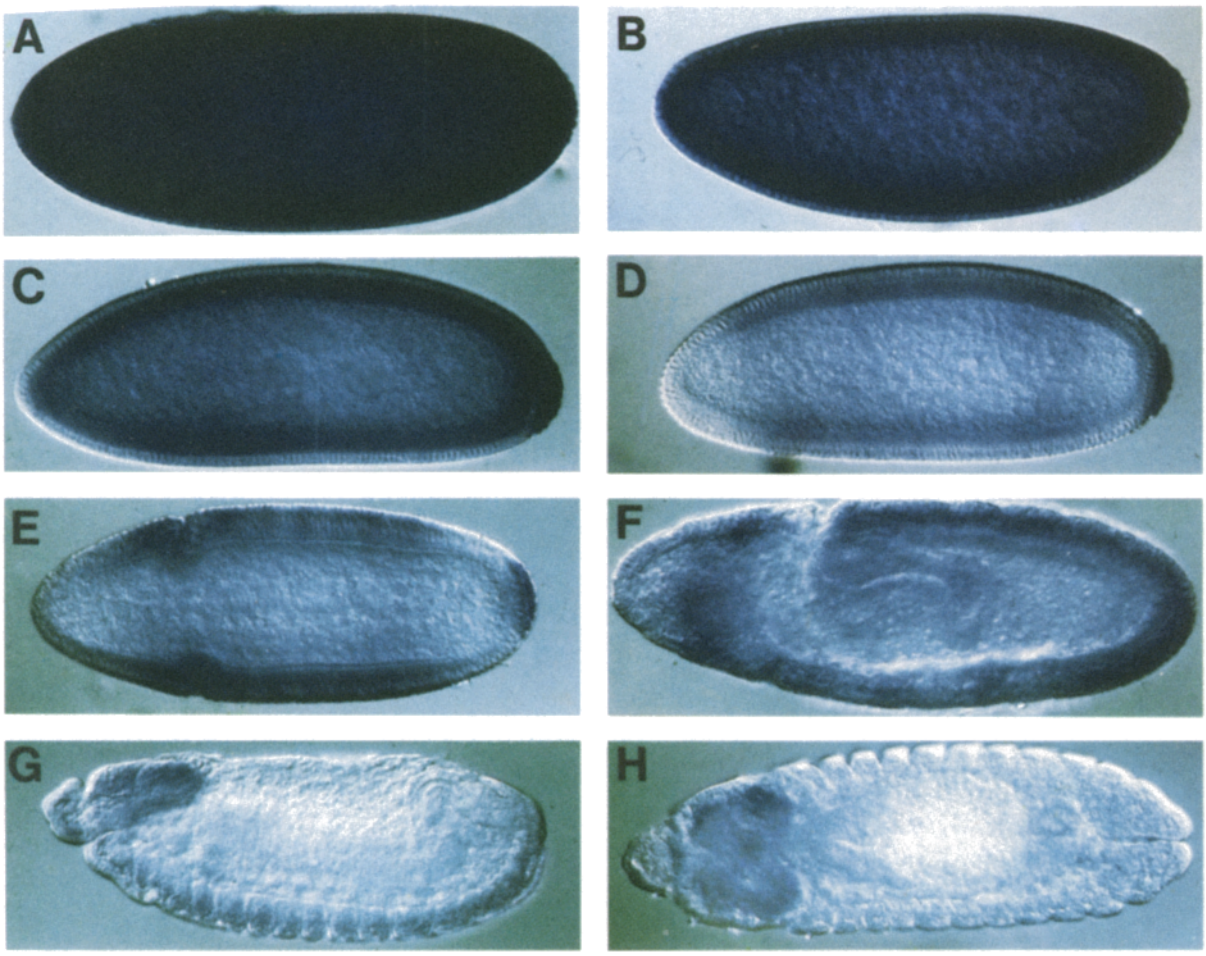

Figure 5. Expression of *oho31* during embryonic development. Whole-mount embryos were hybridized with an *oho31* antisense single-stranded RNA probe labeled by incorporation of digoxigenin-11-dUTP. All embryos are oriented anterior to left and viewed laterally unless otherwise indicated. (*A*) A cleavage stage embryo at the time of pole cell formation, ~80 min after egg deposition (AED), showing a high and uniform level of *oho31* transcripts in the entire embryo. (*B*) An early syncytial blastoderm embryo (mitotic cycle 12), ~100–110 min AED, and (*C*) a syncytial blastoderm embryo (mitotic cycle 13), ~120–130 min AED, showing gradual disappearance of *oho31* transcripts from the yolk and concentration in the cortical cytoplasm. (*D*) A cellular blastoderm embryo, ~140–170 min AED, showing a low level of *oho31* transcripts with a subtle anterior–posterior banded pattern and a concentration of transcripts in the pole cells. (*E*) Dorsal view of an embryo during formation of cephalic folds, ~170–180 min AED, showing distribution of *oho31* transcripts in seven diffuse stripes along the anterior–posterior axis of the embryo, with a higher level of transcripts in the pole cells. (*F*) A germ band extending embryo, ~260–320 min AED, showing higher levels of transcripts in neuroblasts and ventral ectoderm, where they are distributed to diffuse stripes. (*G*) Lateral and (*H*) dorsal views of embryos during germ band shortening, ~560–620 min AED, showing *oho31* transcripts in the supraesophageal ganglions and along the ventral chord.

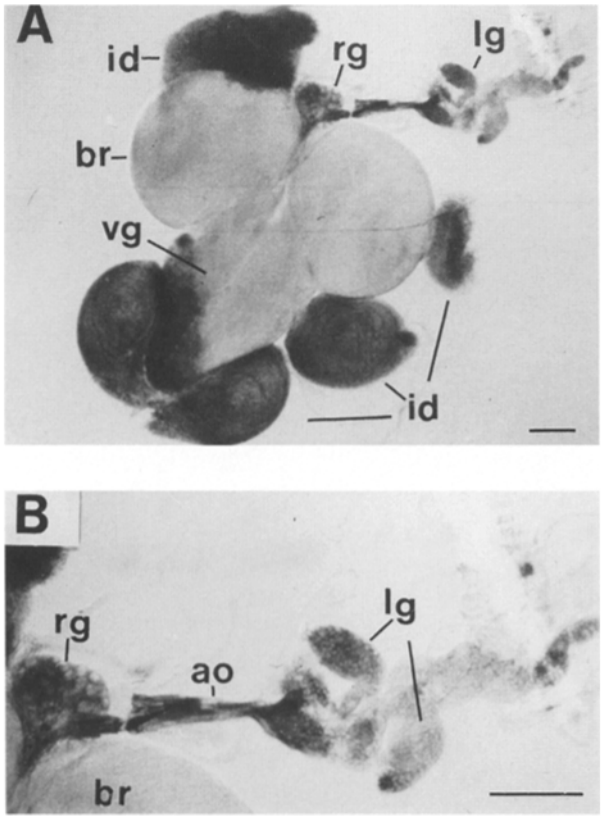

Figure 6. Expression of *oho31* RNA in tissues of third instar larvae. Whole-mount preparations of brain with associated imaginal discs and hematopoietic organs were hybridized with a single-stranded antisense cDNA probe labeled with digoxigenin-11-dUTP. (*A* and *B*) High expression of *oho31* transcripts is detected in the imaginal discs (*id*), and a more moderate expression is seen in the ring gland (*rg*) and the lymph glands (*lg*) associated with the aorta (*ao*). Low level of *oho31* expression can be seen in the brain hemispheres (*br*) and the ventral ganglion (*vg*). *B* shows a higher magnification of the ring gland and the lymph glands than in *A*. Bars: 50 μm.

cated in Fig. 7. This motif is also shared by a series of other proteins (Peifer et al., 1994) and was originally identified in the *Drosophila* segment polarity gene product *armadillo* (Riggleman et al., 1989). Thus, the central domain of *OHO31* spanning amino acids 114–454 consists of eight repeats almost identical in size and probably similar in structure. Furthermore, these eight repeats are relatively rich in hydrophobic amino acids. By contrast, the NH_2- and COOH-terminal regions flanking the central domain are

Table I. Comparison of Protein Sequences Sharing Extensive Similarity with oho31

	OHO31	*RCH-1*	*mSRP1*	*SRP1*	*IMP*
OHO31		50.8	45.2	42.1	49.7
RCH-1	69.3		46.6	45.7	62.6
mSRP1	64.9	64.7		52.7	45.4
SRP1	62.8	62.8	70.9		49.7
IMP	70.0	76.8	66.4	70.0	

Above the diagonal is reported the percentage sequence identity; below the diagonal is indicated the percentage sequence similarity if conservative substitutions are counted. *IMP, Importin.*

```
  1 MDNGTDSSTSKFVPEYRRTNFKNKGRFSADELRRRRDTQQVELRKAKRDEALAKRRNFIP      SRP1
  1 -----MSTPGK--ENFRLKSYKNKS-LNPDEMRRRREEEGLQLRKCKREEQLFKRRNV--     MSRP1
  1 ----MC-TNENALPAARLNRFKNKGKDST-EMRRRRIEVNVELRKAKKDDQMLKRRNVSS     RCH1
  1 ----MPTTNEADE---RMRKFKNKGKDTA-ELRRRRVEVSVELRKAKKDEQILKRRNVC-     IMP1
  1 --------MSKADSNSRQGSYKANS-INTQDSDRRRHEVTIELRKSKKEDQMFKRRNIND     OHO31

 61 PTDGAD-SDEEDESSVSADQQFYSQLQQELPQMTQQLN--SD--DMQ-----EQ-LSATVKFRQI  SRP1
 50 ----AT-AEEETEEEVMSDGGFHEA-QINNMEMAPGGVITSDMTDMIFSNSPEQQLSATQKFRKL  MSRP
 55 FPDDAT-SPLQENRNNQGTVNW------SVDDIVKGIN--SS--NVE-----NQ-LQATQAARKL  RCH1
 52 LPEELILSPEKNAMQSVQVPPL------SLEEIVQGMN--SG--DPE-----NE-LRCTQAARKM  IMP1
 52 --EDLT-SPLKE-LNGQSPVQL------SVDEIVAAMN--SE--DQE-----RQ-FLGMQSARKM  OHO3

115       LSREHRPPIDV---VIQ-AGVVPRLVEFMRENQPEMLQL---EAAWALTN            SRP1
110       LSKEPNPPIDE---VINTPGVVARFVEFLKRKENCTLQF---ESAWVLTN            MSRP1
103       LSREKQPPIDN---IIR-AGLIPKFVSFLGRTDCSPIQF---ESAWALTN            RCH1
111       LSRERNPPLND---IIE-AGLIPKLVEPLSRHDNSTLQP---EAAWALTN            IMP1
 97       LSRERNPPIDL---MIG-HGIVPICIRFLQNTNNSMLQF---EAAWALTN            OHO31

158       IASGTSAQTKV---VVD-ADAVPLFIQLLYTGSVEVKE----QAIWALGN            SRP1
154       IASGNSLQTRN---VIQ-AGAVPIFIELLSSEFEDVQE----QAVWALGN            MSRP1
146       IASGTSEQTKA---VVD-GGAIPAFISLLASPHAHISE----QAVWALGN            RCH1
154       IASGTSDQTKS---VVD-GGAIPAFISLISSPHLHISE----QAVWALGN            IMP1
140       IASGTSDQTRC---VIE-HNAVPHFVALLQSKSMNLAE----QAVWALGN            OHO31

200       VAGDSTDYRDY---VLQCNAMEPILGLFNSNKP-SLIR----TATWTLSN            SRP1
196       IAGDSTMCRDY---VLNC-ILPPLLQLFSKQNRLTMTR----NAVWALSN            MSRP1
189       IAGDGSVFRDL---VIKYGAVDPLLALLAVPDMSSLACGYLRNLTWTLSN            RCH1
196       IAGDGPLYRDA---LINCNVIPPLLAL--VNPQTPL--GYLRNITWMLSN            IMP1
182       IAGDGAAARDI---VIHHNVIDGILPLINNETPLSFLR----NIVWLMSN            OHO31

242       LCRGKKPQPDW---SVV-SQALPTLAKLIYSMDTETLV----DACWAISY            SRP1
239       LCRGKSPPPEF---AKV-SPCLNVLSWLLFVSDTDVLA----DACWALSY            MSRP1
235       LCRNKNPAPPI---DAV-EQILPTLVRLLHHDDPEVLA----DTCWAISY            RCH1
239       LCRNKNPYPPM---SAV-LQILPVLTQLMHHDDKDILS----DTCWAMSY            IMP1
225       LCRNKNPSPPF---DQV-KRLLPVLSQLLLSQDIQVLA----DACWALSY            OHO31

284       LSDGPQEAIQA---VID-VRIPKRLVELLSHESTLVQT----PALRAVGN            SRP1
281       LSDGPNDKIQA---VID-AGVCRRLVELLMHNDYKVVS----PALRAVGN            MSRP1
277       LTDGPNERIGM---VVK-TGVVPQLVKLLGASELPIVT----PALRAIGN            RCH1
281       LTDGSNDRIDV---VVK-TGIVDRLIQLMYSPELSIVT----PSLRTVGN            IMP1
267       VTDDDNTKIQA---VVD-SDAVPRLVKLLQMDEPSIIV----PALRSVGN            OHO31

326       IVTGNDLQTQV---VIN-AGVLPALRLLLSSPKENIKK----EACWTISN            SRP1
323       IVTGDDIQTQV---ILN-CSALQSLLHLLSSPKESIKK----EACWTISN            MSRP1
319       IVTGTDEQTQV---VID-AGALAVFPSLLTNPKTNIQK----EATWTMSN            RCH1
323       IVTGTDKQTQA---AID-AGVLSVLPQLLRHQKPSIQK----EAAWAISN            IMP1
309       IVTGTDQQTDV---VIA-SGGLPRLGLLLQHNKSNIVK----EAAWTVSN            OHO31

368       ITAGNTEQIQA---VID-ANLIPPLVKLLEVAEYKTKK----EACWAISN            SRP1
365       ITAGNRAQIQT---VID-ANMFPALISILQTAEFRTRK----EAAWAITN            MSRP1
361       ITAGRQDQIQQ---VVN-HGLVPFLVSVLSKADFKTQK----EAVWAVTN            RCH1
365       IAAGPAPQIQQ---MIT-CGLLSPLVDLLNKGDFKAQK----EAVWAVTN            IMP1
351       ITAGNQKQIQA---VIQ-AGIFQQLRTVLEKGDFKAQK----EAAWAVTN            OHO31

410       ASSGGLQRPDIIRYLVS-QGCIKPLCDLLEIADNRIIE----VTLDALEN            SRP1
407       ATSGG--SAEQIKYLVE-LGCIKPLCDLLTVMDAKIVQ----VALNGLEN            MSRP1
403       YTSGG--TVEQIVYLVH-CGIIEPLMNLLTAKDTKIIL----VILDAISN            RCH1
407       YTSGG--TVEQVVQLVQ-CGVLEPLLNLLTIKDSKTIL----VILDAISN            IMP1
393       TTTSG--TPEQIVDLIEKYKILKPFIDLLDTKDPRTIK----VVQTGLSN            OHO31

455 ILKMGEADKEARGLNINENADFIEKAGGMEKIFNCQQNENDKIYEKAYKIIETYFG-EEE      SRP1
450 ILRLGEQEAKRNGSGINPYCALIEEAYGLDKIEFLQSHENQEIYQKAFDLIEHYFGTEDE      MSRP1
447 IFQAAEKLGETEKLSI-----MIEECGGLDKIEALQNHENESVYKASLSLIEKYFSVEEE      RCH1
450 IFLAAEKLGEQEKL-----CLLVEELGGLEKIEALQTHDNHMVYHAALALIEKYFSGEEA      IMP1
437 LFALAEKLGGTENL-----CLMVEEMGGLDKLETLQQHENEEVYKKAYAIIDTYFSNGDD      OHO31

514 DAVDETMAPQNAGN----TFGFGSNVNQQFNPN 542                             SRP1
510 D---SSIAPQVDLSQQQYIPQQCEAPMEGFLQ- 538                            MSRP1
502 ED--QNVVPETTSEGY--TFQVQDGAPGTFNF- 529                            RCH1
505 DD--IALEPEMGKDAY--TFQVPNMQKESFNF- 528                            IMP1
491 EAEQEL-APQEVNGALEFNATQPKAPEGGYTF- 522                            OHO31

          I       Q    I    II  I     D  I      E   IS
Consensus L  G   Q D ---VV - GLLP LL LL   E  V  ----DA WALGN
 repeat                    VV   V                    VT
```

Figure 7. Amino acid sequence comparison of the *Drosophila OHO31* protein with the yeast *SRP1* protein, the *Importin* protein of *Xenopus*, and two mammalian homologues, *mSRP1* and *RCH1*. Alignment of these proteins was performed by using the BESTFIT and MULTIALIGN programs. Gaps indicated by dots were introduced to facilitate alignment. The eight internal *arm* repeats are also aligned, and a consensus sequence for the internal repeat structure based on the repeats from the five proteins is depicted. A cluster of conserved basic residues forming a potential bipartite nuclear targeting sequence is boxed in the NH_2-terminal region of these proteins.

highly hydrophilic, with several clusters of acidic and basic amino acids. In particular, there are 6 acidic and 14 basic amino acids in the first 50 residues covering the NH_2-terminal region, whereas the COOH-terminal region between residues 437 and 522 contains 18 acidic and 6 basic amino acid residues. No obvious secretory signal sequence is present, suggesting that the *OHO31* protein may act intracellularly.

Characterization of Anti-OHO31 Antibodies

To analyze the expression of the *OHO31* protein, we raised antibodies against a bacterially produced *OHO31* fusion protein. We purified anti-*OHO31* antibodies by affinity chromatography and preadsorption to protein extracts of homozygous lethal *oho31*^{D14} larvae in which the coding sequence of *oho31* is partially deleted. The specificity of the recovered anti-*OHO31* antibodies was analyzed by immunoblotting experiments. As shown in Fig. 8 *A*, the anti-*OHO31* antibodies reacted exclusively with a single 58-kD protein in a protein extract of brain and imaginal discs of wild-type late third instar larvae. A protein of similar size was only weakly detected in an extract of homozygous *oho31*$^{144\text{-}1}$ mutant larvae, and no protein was found in an extract of homozygous *oho31*^{D14} larvae. Without preadsorption, the anti-*OHO31* antibodies gave rise to a similar staining pattern, albeit detecting additional faint bands in all three protein extracts (data not shown). These results demonstrate that the anti-*OHO31* antibodies are specific for the *OHO31* protein; no cross-reaction with other proteins is evident. They also confirm that the insertion of the P element reduces considerably the expression of *OHO31* in the *oho31*$^{144\text{-}1}$ mutant.

Developmental Pattern of Expression and Phosphorylation of the OHO31 Protein

In vitro translation of the cDNA *K2* in a coupled transcription–translation reticulocyte lysate system using T3 RNA polymerase produced a single [^{35}S]methionine-labeled polypeptide with an apparent molecular mass of ~58 kD corresponding to the calculated molecular weight of the *OHO31* protein (Fig. 8 *B*). By contrast, immunoblot analysis revealed that the *OHO31* protein observed during different stages of *Drosophila* development can be resolved into at least two species by SDS-PAGE: a faster and a slower migrating species (Fig. 8 *B*, lanes *IP* and *b.IP*, and *C*, *b*). The faster migrating species displayed a similar size as the in vitro translated *OHO31* protein. Although the level of faster migrating protein varied dramatically during development, it was seen during all developmental stages. High levels of this protein were detected in early embryos and ovaries; moderate levels were found in all the other developmental stages with the exception of larval development, where the *OHO31* protein was only present at a very low level and would have remained virtually unnoticed if we were not examining brain and imaginal disc preparations as shown in Fig. 8 *A*. By contrast, the slower migrating species was only detected in ovaries and preblastoderm embryos, where it reached a similar level of expression as the faster migrating species.

Since slower migration of proteins in SDS-PAGE is often observed with the phosphorylated forms of polypep-

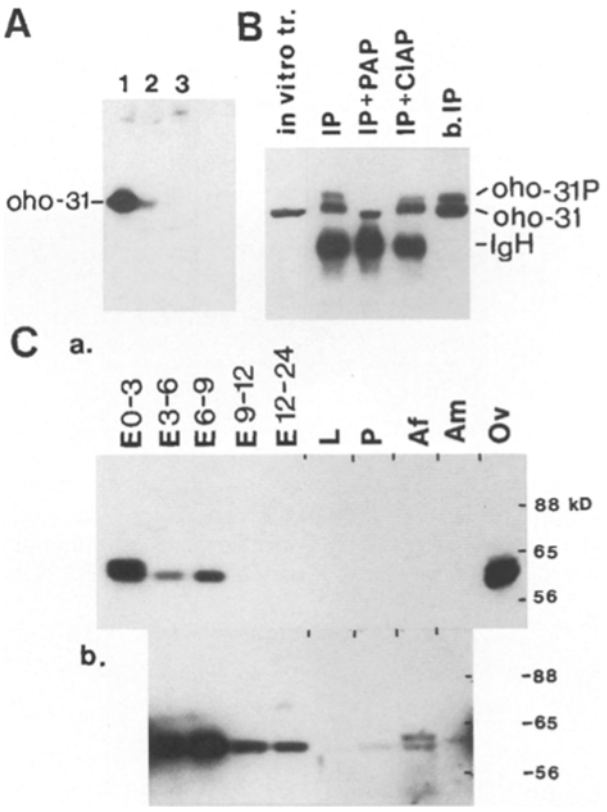

Figure 8. OHO31 protein expression in various genotypes and throughout development in wild-type animals, and phosphatase treatment. (*A*) *OHO31* protein expression in larval tissues of different genotypes. Proteins extracted of brain and imaginal discs from wild-type (lane *1*), homozygous *oho31*$^{144/1}$ (lane *2*), and homozygous *oho31*^{D14} (lane *3*) third instar larvae were resolved on a 7% polyacrylamide gel and transferred to a PVDF membrane. The protein blot was probed with affinity-purified anti-*OHO31* antibodies. The amount of proteins in the different lanes was first equalized by comparing aliquots in a Coomassie blue–stained gel. (*B*) Phosphatase treatments of *OHO31* protein. Immunoprecipitation of *OHO31* proteins extracted from wild-type embryos (0–3 h AED) was performed using anti-*OHO31* antibodies and protein A–Sepharose. One third of the immunoprecipitated sample was treated with PAP (*IP+PAP*), another third was treated with CIAP (*IP+CIAP*), and the last third was treated identically to the PAP-treated sample except that the enzyme was omitted (*IP*). The immunoprecipitated proteins were resolved on a 7% polyacrylamide gel. On the same gel (*b.IP*), total embryonic proteins were also separated, as well as (in vitro tr.) [^{35}S]methionine-labeled *OHO31* protein translated in an in vitro transcription–translation coupled reticulocyte system with *oho31 K2* cDNA as template. After gel electrophoresis, the proteins were transferred to a PVDF membrane. The protein blot was sequentially exposed to an autoradiogram, first for detecting the in vitro translated *OHO31* protein, and then probed with affinity-purified anti-*OHO31* antibodies for detecting the *OHO31* proteins. Positions of Ig heavy chain and underphosphorylated and hyperphosphorylated forms of *OHO31* are indicated by IgH, oho-31, and oho-31P, respectively. (*C*) Developmental profile of *OHO31* protein expression. Immunodetection of *OHO31* proteins in extracts from embryonic (*E* of 0–3, 3–6, 6–9, 9–12, and 12–24 h AED), larval (*L*) and pupal (*P*) stages, adult males (*Am*), adult females (*Af*), and ovaries of 3-d-old females (*Ov*). Proteins were separated on a 7% polyacylamide gel and transferred to a PVDF membrane, which was probed with affinity-purified anti-*OHO31* antibodies using the Tropix chemoluminescence system. *b* shows a longer exposure of the immunoblot displayed in *a*.

tides, we tested whether the changes in mobility were due to the presence of phosphate on *OHO31* protein. Immunoprecipitated *OHO31* proteins extracted from early embryos were treated with acidic and alkaline phosphatases. As shown in Fig. 8 *A*, treatment with PAP caused all of the *OHO31* protein to comigrate as a single species with a relative molecular mass equivalent to that of the faster migrating form, whereas treatment with CIAP converted only a portion of the slower migrating form into the faster migrating form. Addition of orthophosphate to the *OHO31* immunocomplexes inhibited the phosphatase-mediated shift in molecular mass (data not shown). These data indicated that the polypeptides with a slower migration rate were phosphorylated forms of the *OHO31* protein.

Similar to the results of the developmental Northern blot analysis, the immunoblotting data showed that the expression of *OHO31* proteins was at its highest during early embryogenesis. The high level of *OHO31* proteins found in early embryos should represent the accumulation of maternally synthesized proteins as judged by the high level of *OHO31* protein found in ovaries as well as embryonic proteins synthesized from maternally produced transcripts (Fig. 5). Furthermore, the rapid reduction in the levels of *OHO31* protein during early embryogenesis suggests that *OHO31* decay is correlated with mitotic activity in the embryo.

During Early Embryogenesis the OHO31 Protein is Accumulating in the Nucleus in a Cell Cycle–dependent Fashion

To monitor the temporal changes in *OHO31* distribution during embryogenesis, we performed immunochemical staining using a color reaction that allowed us to visualize the relative amount of *OHO31* in different regions of the embryos or in different subcellular compartments.

As expected from the high level of *OHO31* proteins seen on immunoblots, an intense immunostaining signal was detected in preblastoderm embryos (Fig. 9). In the majority of the examined embryos, the distribution of *OHO31* appears uniform, and its level remains constant during the early syncytial cell cycles (mitoses 1–8). When the nuclei migrate to the periphery, the *OHO31* protein is predominantly located in the periplasm (Fig. 9 *C*), and its level declines progressively during the subsequent nuclear cycles (mitoses 9–13), so that by early gastrulation, the *OHO31* protein is present but only at a low level.

However, in a minority of embryos, ~5%, we noticed a spotted pattern of anti-*OHO31* staining that we attributed to a transient accumulation of the *OHO31* protein in the nuclei. This accumulation could be seen in preblastoderm embryos with the energids more stained than the ooplasm, as shown for mitoses 3, 8, and 9 in Fig. 9, *B–D*, respectively. The nuclear staining then became more visible during the syncytial blastoderm stages when the nuclei are aligned under the cortical surface and are thus more accessible to optical examination (Fig. 9, *D–I*). Additional changes in *OHO31* distribution can also be noticed during the syncytial blastoderm. The staining appears graded from posterior to anterior, with almost no staining at the anterior end and the strongest staining at the posterior end of the embryo, where it forms a cap underlying the pole cells. However, the pole cells are themselves devoid of *OHO31* proteins despite the relatively high abundance *oho31* mRNA present in these cells, as shown in Fig. 5. In these cells, inhibition of the translation of *oho31* mRNA may result from the presence of a *nanos*-responsive element at the 3′ end of the mRNA (Wharton and Struhl, 1991; Dalby and Glover, 1992). During gastrulation and germ band extension, the *OHO31* protein was essentially present in the ventral ectodermal neurogenic region, as shown in Fig. 9 *J*, and in the ventral chord (data not shown) and was diffusely distributed in the cytoplasm of these tissues.

OHO31 Protein Accumulates in the Nucleus at the Onset of Mitosis

To study the mitotic behavior of the *OHO31* protein during the cell cycle, we further stained whole-mount preparations of early wild-type embryos with propidium iodide to visualize DNA and FITC-conjugated antibodies to visualize the *OHO31* protein and examined the embryos with a confocal laser scanning microscope.

As shown in Fig. 10, the intensity of the nuclear staining for the *OHO31* protein varied during the cell cycle, with maximal staining occurring at the onset of mitosis during prophase. Then the nuclear staining regressed dramatically with the progression of mitosis. In anaphase, the level of nuclear staining was comparable to that of the cytoplasm. At the end of mitosis, the level of nuclear staining increased moderately and then remained constant during interphase up to the onset of the next mitosis.

Although the level of nuclear staining for *OHO31* increased with chromatid condensation, *OHO31* remained apparently free from a direct association with the chromosomes, as indicated by the pattern of nuclear staining for *OHO31*, which is complementary to the pattern of DNA staining. In addition, the *OHO31* protein was not concentrated at the nuclear periphery, as can be seen for nuclear envelope proteins, such as lamins (Fuchs et al., 1983; Smith and Fisher, 1984; Frasch et al., 1988; data not shown).

The strong regression of nuclear staining for *OHO31* during anaphase and telophase, resulting in a faint shadow over the condensed chromosomes and the equatorial plate, suggests that the *OHO31* protein is either degraded in the nucleus during metaphase, redistributed in the cytoplasm as the nuclear membrane is ruptured, or inaccessible to the antibodies. However, the rate of disappearance of anti-*OHO31* staining during the 13 nuclear divisions taking place during early embryogenesis appeared to increase with the cumulative number of mitoses, indicating that the degradation of *OHO31* may be an active nuclear process.

Discussion

We have identified a component involved in the regulation of cell proliferation by cloning the *oho31* gene, whose inactivation in *Drosophila* leads to the malignant transformation of the hematopoietic organs and the genital disc. Our analysis of the distribution of the *OHO31* protein in wild-type embryos revealed that the intracellular localization of this protein changes dramatically during the cell cy-

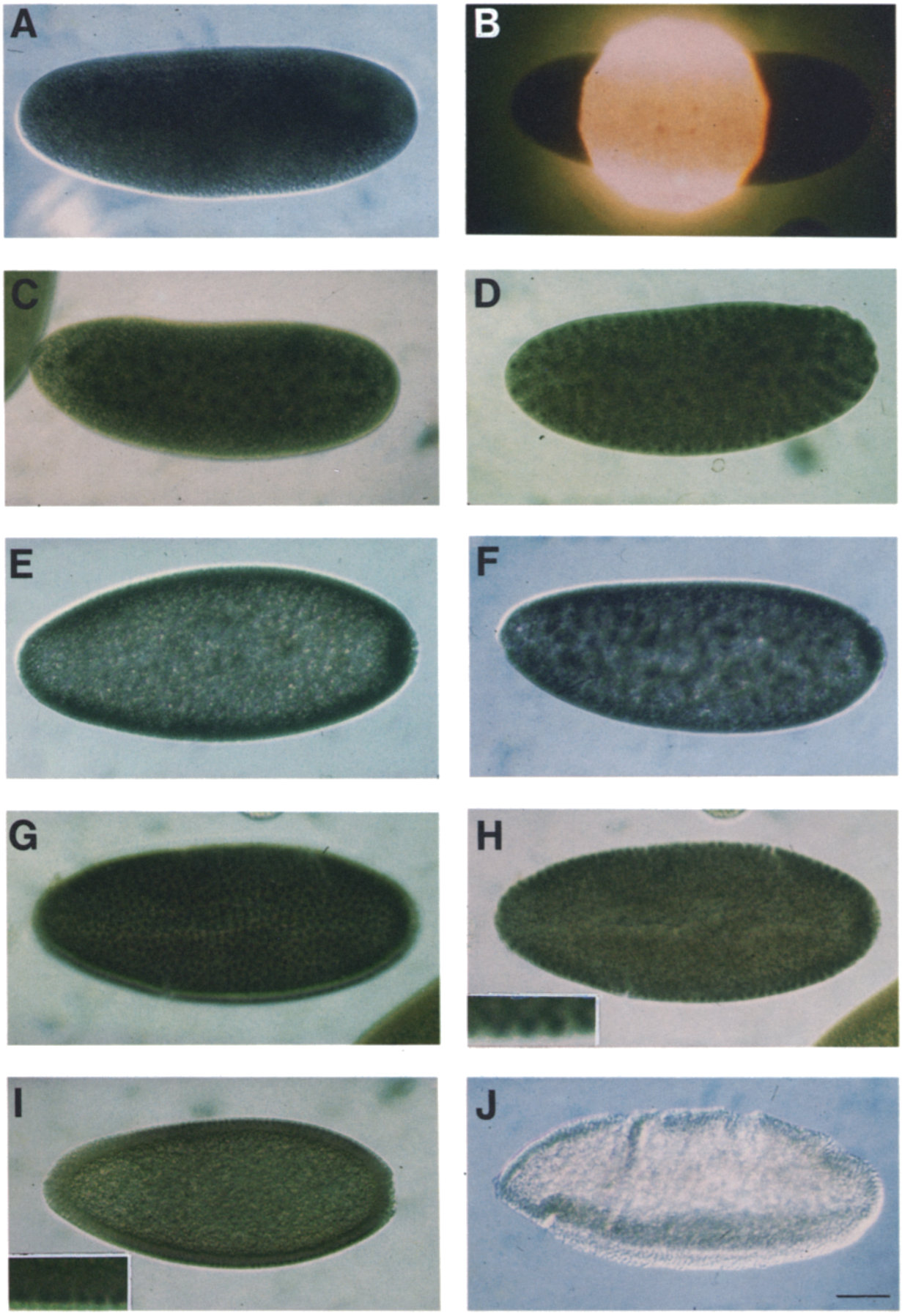
A
B
C
D
E
F
G
H
I
J

cle. During the first 13 mitotic cycles that occur synchronously in a shared cytoplasm, we found that the *OHO31* protein is basically localized in the cytoplasm but accumulates transiently in the nucleus at the beginning of mitosis, a key transition point of the cell cycle. The relocalization of *OHO31* in the nucleus indicates that this protein may play a direct role in the regulation of cell division, although the exact nature of this mechanism remains to be determined. Taking into account the recent finding that the *Importin* protein of *Xenopus* acts as a carrier for the import of karyophilic proteins into the nucleus (Görlich et al., 1994), we propose that the *OHO31* protein, which is closely related to *Importin*, exhibits a similar function. Thus the *oho31* gene encodes the first example of a tumor suppressor involved in nuclear protein import.

Tumors Arise from Inactivation of the oho31 Gene

The most dramatic effect resulting from the inactivation of the *oho31* gene in *Drosophila* is certainly the overgrowth of a series of imaginal organs. Our molecular analysis shows that both the strong hypomorphic mutation induced by the P element insertion in the promoter region of the *oho31* gene and the two amorphic mutations caused by the imprecise excision of this P element give rise to lethal larvae displaying an identical phenotype. Based on this criterion, the *oho31* gene can be classified as a true tumor suppressor gene.

Inactivation of the *oho31* gene gives rise to a pleiotropic pattern of tissue overgrowth ranging from a moderate hyperplasia of the imaginal rings of the salivary glands, whose size increases but whose structure remains apparently normal, to malignant neoplasia of the hematopoietic organs and the genital disc. These two tissues expand massively and, after transplantation into adult hosts, can grow autonomously. However, the low rate of growth of the implants suggests that the malignant potential of the tumorous *oho31* cells may revert during the growth of these cells. In particular, we found that the hemocytic tumors and the successfully growing implants derived from them consist of well-differentiated hemocytes. We can thus infer that the uncontrolled growth of the hemocytes in *oho31*-mutant animals is a temporary phenomenon occurring at an early stage of their differentiation. Successful transplantation may occur when the implant contains cells at a defined, presumably earlier, phase of their differentiation. Since we have transplanted cells from relatively large tumorous masses found in old surviving larvae, it is possible that the majority of the cells were already too advanced in their differentiation to form secondary tumors. Together, these data suggest that *oho31* inactivation may extend the period of cell proliferation in a series of organs by delaying the progression of normal cell differentiation.

Structural Similarities among OHO31-like Proteins

The *OHO31* protein displays strong structural similarity to a family of four proteins including the *Importin* protein of *Xenopus*, a cytosolic factor in nuclear import (Görlich et al., 1994), the yeast nucleopore complex–associated *SRP1* protein (Yano et al., 1992), as well as the mammalian *hSRP1* (and *mSRP1*) (Cortes et al., 1994) and *RCH-1* proteins (Cuomo et al., 1994). The finding that the two mammalian proteins are as distantly related to each other as they are divergent from their yeast, insect, and amphibian homologues indicates that *OHO31* is a member of a larger family of proteins with related function. This also suggests that the yeast and vertebrate relative closest to *OHO31* may need yet to be identified. Moreover, on the basis of the divergence between the members of the family of *OHO31* proteins, it would not be surprising that further homologues may exist in the genome of *Drosophila.* The identification of such homologues and the study of their spatio-temporal expression and coordination may provide further clues on the function of *OHO31*-like proteins.

The most conserved region among the *OHO31*-like proteins is the central domain made of eight degenerate repeats displaying significant homologies with the *arm* motif (Riggleman et al., 1989) ascertained in a number of other proteins (Peifer et al., 1994). In addition to the members of the *OHO31*-like proteins, *arm* motifs were found in *armadillo*'s mammalian homologues, the adhesive junction proteins β-catenin (McCrea et al., 1991) and plakoglobin (Franke et al., 1989), p120, a protein-tyrosine kinase substrate present in cell–cell junctions (Reynolds et al., 1992), and smsGDS, an exchange factor for Ras-related G proteins (Kikuchi et al., 1992). Furthermore, the *arm* motif was also identified in the human tumor suppressor *adenomatous polyposis coli* (Kinzler et al., 1991; Groden et al., 1991).

Recent findings indicate the *arm* domains may be the site of interaction with other proteins. Genetic evidence indicates that the *arm* repeats of the yeast *SRP1* protein is the site of interaction with the zinc finger domain of the two subunits A190 and A135 of RNA polymerase I, since the *SRP1 arm* repeats contain the mutation suppressing the RNA polymerase I temperature-sensitive mutations (Yano et al., 1992). Deletion mapping of *hSRP1* and *RAG-1* interacting domains using the yeast two-hybrid system showed that a region containing at least four *arm* repeats in *hSRP1* is required for interaction with *RAG-1* (Cortes et al., 1994). Further genetic and immunological

Figure 9. Localization of the *OHO31* protein during *Drosophila* embryogenesis. All embryos are oriented anterior to left and ventral side down. *OHO31* proteins were localized by a color reaction after staining with affinity-purified anti-*OHO31* antibodies. (*A*) A preblastoderm embryo at mitosis 3 showing a high and uniform distribution of *OHO31*, but (*B*) displaying a more intense staining in the four nuclei located in the center of the embryo as examined under a stronger illumination and a reduced field. Preblastoderm embryos at mitosis 8 (*C*) and 9 (*D*) showing accumulation of *OHO31* protein in the nuclei. (*E*) A syncytial blastoderm embryo during interphase of cell cycle 10 showing a diffuse and uniform distribution of *OHO31* protein in the periplasm. (*F*) A syncytial blastoderm embryo at mitosis 10. A syncytial blastoderm embryo at mitosis 11 with the plane of focus at the surface (*G*) or the center (*H*) of the embryo. (*I*) An embryo at mitosis 12. Insets in both *H* and *I* display enlargements of the cortical periplasm where *OHO31* protein accumulates in the mitotic nuclei. (*J*) Gastrulating embryo showing accumulation of *OHO31* protein in the cells of the ventral ectodermal neurogenic region. Embryos stained with secondary antibodies alone showed no staining (data not shown).

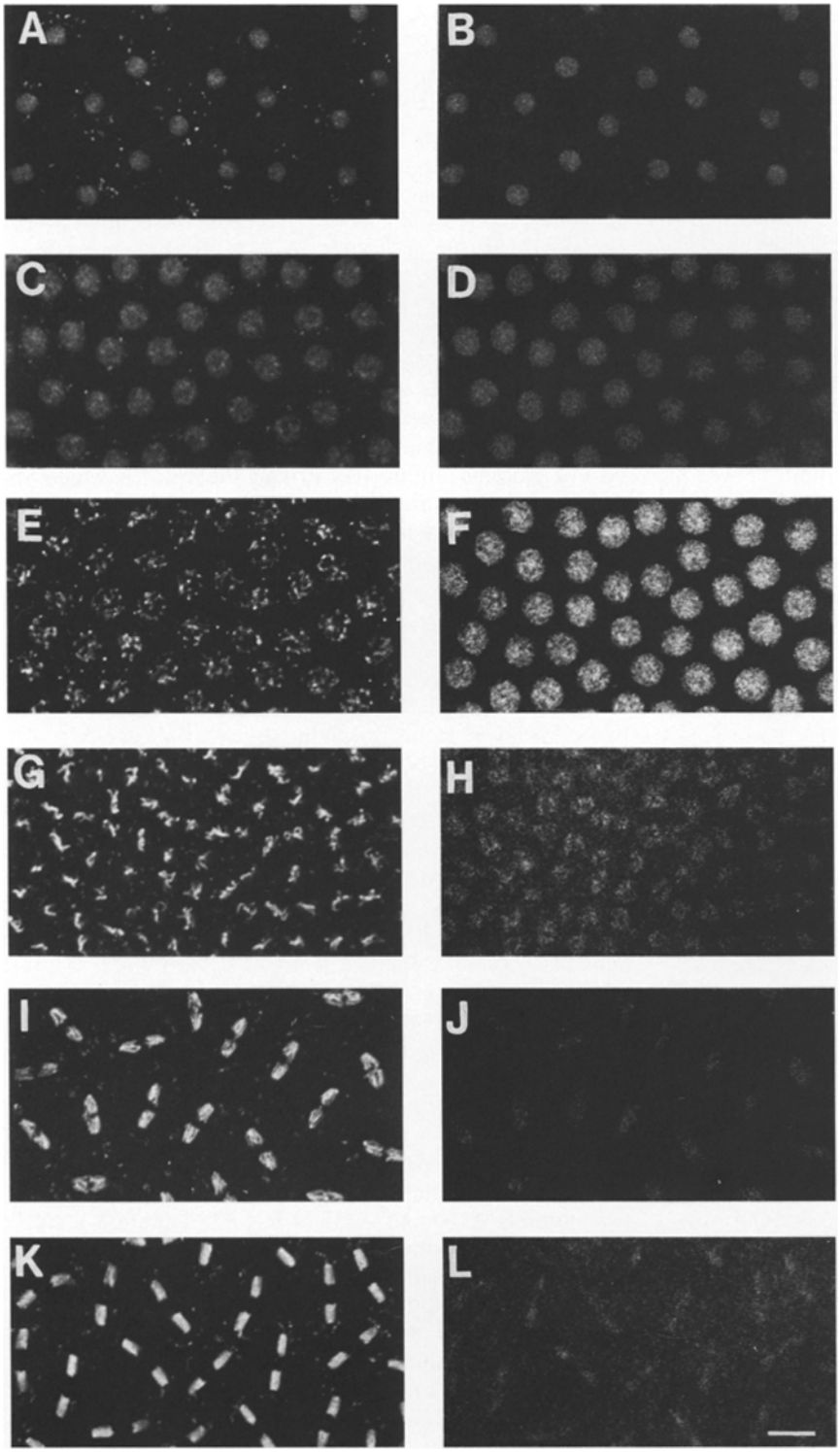

Figure 10. Behavior of the *OHO31* protein during early embryonic mitoses. Wild-type embryos were double stained for DNA (*A*, *C*, *E*, *G*, *I*, and *K*) with propidium iodide and for *OHO31* proteins (*B*, *D*, *F*, *H*, *J*, and *L*) with anti-*OHO31* antibodies and FITC-conjugated secondary antibodies as described in Materials and Methods. Confocal images from embryos at interphase of nuclear cycle 10 (*A* and *B*), late interphase of nuclear cycle 11 (*C* and *D*), prophase of nuclear cycle 11 (*E* and *F*), metaphase of nuclear cycle 12 (*G* and *H*), anaphase of nuclear cycle 10 (*I* and *J*), and telophase of nuclear cycle 10 (*K* and *L*) showing the transitory nuclear accumulation of *OHO31* during prophase. Control embryos stained only with the FITC-conjugated secondary antibodies showed no staining above background level. Bar: 10 μm.

studies revealed that the binding of *SRP1* to nucleopore complex proteins *NUP1* and *NUP2* is mediated through the central repetitive domain of these proteins (Belanger et al., 1994). These results suggest that *SRP1* and its mammalian homologues bind nuclear proteins (Yano et al., 1992; Cuomo et al., 1994; Belanger et al., 1994; Cortes et al., 1994), in a similar way as the junctional proteins containing *arm* repeats may link cytoskeletal elements at intercellular junctions by mediating strong protein–protein interaction (for review see Kemler, 1993; Peifer et al., 1994).

Although the NH_2- and COOH-terminal domains of the *OHO31*-like proteins are less conserved, we noticed a segment of 24 amino acids **RRRR**$(x)_7$**RK**x**KK**$(x)_5$**KRR** containing 11 basic residues, of which 10 (bold letters) are conserved. In *OHO31*, the row of four arginines present in this motif is disrupted by the replacement of a methionine residue at amino acid position 25 (**R**^{24}**M**RR-HEVTIEL**RKSKK**EDQMF**KRR**^{47}). The NH_2-terminal moiety of this motif is reminiscent of the bipartite nuclear localizing sequence **KR**$(x)_{10}$**KKKK** identified in nucleoplasmin (Dingwall et al., 1988) and other nuclear proteins,

such as the glucocorticoid and estrogen receptors (Picard and Yamamoto, 1987; Picard et al., 1990; Robbins et al., 1991). The presence of such a basic motif is intriguing because a recent model proposes that *Importin* and a rat protein homologous to *hSRP1* may act as cytosolic receptors for nuclear localizing sequence–containing proteins (Powers and Forbes, 1994). Thus, it would be interesting to determine whether the basic motif conserved in the NH_2-terminal region of the *OHO31*-like proteins may play a direct role in their nuclear import.

Nuclear Import of OHO31

The *OHO31*-like proteins appear to fulfill analogous functions in nucleocytoplasmic exchanges of a variety of macromolecules such as proteins, RNPs, and so on. The recent description and cloning of the *Importin* protein of *Xenopus* shed new light on the role of these proteins as cytosolic factors involved in nuclear protein import. Purified *Importin* was shown to elicit binding of karyophylic proteins to the nuclear envelope of permeabilized cells and to mediate nuclear translocation of such proteins in conjunction with Ran/TC4 and an energy-regenerating system (Görlich et al., 1994).

The yeast *srp1* gene was originally identified as a suppressor of temperature-sensitive mutations of RNA polymerase I and characterized as an essential gene for cell viability (Yano et al., 1992). Inactivation of the *srp1* gene in *Saccharomyces cerevisiae* results in arrest of transcription, breakup of the nucleolus, and defects in both nuclear division and segregation. Immunobiochemical analyses showed that the *SRP1* protein can be physically and functionally associated with the nuclear pore complex (Yano et al., 1992, 1994; Belanger et al., 1994). In particular, the *SRP1* protein was found to colocalize with the nucleoporin *Nup1* in immunofluorescence microscopy (Yano et al., 1992), to interact with *NuP1* in a two-hybrid system, and to coimmunoprecipitate with nucleoporins *Nup1* or *Nup2* (Belanger et al., 1994). Moreover, the *srp1* gene was shown to interact genetically with the *nup1* (Belanger et al., 1994) and *nup2* genes (Yano et al., 1994). Furthermore, the *SRP1* protein was also recovered in a soluble fraction, indicating that *SRP1* is also dispersed in the cytoplasm (Yano et al., 1992; Belanger et al., 1994). The presence of *SRP1* in both the cytoplasm and nucleus and the pleiotropic phenotypes of mutations in *srp1* support the contention that *SRP1* may play a role in nucleocytoplasmic transport similar to that of *Importin*. By analogy, the specific interaction of both *hSRP1* and *RCH-1* with *RAG1* (Cuomo et al., 1994; Cortes et al., 1994), which appears to be localized at the nuclear periphery and contains a karyophilic sequence, suggests that the two mammalian homologues may also participate in nucleocytoplasmic transport.

Although the exact function of the *OHO31* protein remains to be elucidated, it is possible to infer from our results that *OHO31* is also involved in nucleocytoplasmic transport. We can show that *OHO31* accumulates in the nucleus during prophase when the nuclear membrane is apparently still intact. Since, in syncytial *Drosophila* embryos, the nuclear envelope is only partially ruptured at the poles at the beginning of metaphase (Stafstrom and Staehelin, 1984; Harel et al., 1989; Foe et al., 1993), the nuclear accumulation of *OHO31* during prophase may reflect an active transport process requiring intact nuclear pores.

The rapid disappearance of *OHO31* from the nucleus during metaphase either reflects a passive dispersion of this protein in the cytoplasm resulting from the rupture of the nuclear envelope or is indicative of a rapid degradation taking place in the nucleus. For two reasons, we favor the latter hypothesis. First, we noted that the rate of *OHO31* decay follows the cumulative number of mitoses occurring during the first 13 nuclear divisions, and second, we consistently detected a higher concentration of *OHO31* in the cytoplasm than in the nucleus of embryonic cells after cell cycle 14 and larval cells expressing *OHO31* at all stages of their cell cycle (data not shown).

The nuclear accumulation of *OHO31* that we observe at prophase in syncytial embryos may reflect the rapid import of proteins required for driving the mitoses, which occur at relatively short intervals in the syncytial blastoderm. This accumulation is consistent with the availability of large maternal stockpiles of both *OHO31* proteins and karyophylic proteins present in the egg, which can be readily recruited into the nucleus at the onset of mitosis. By contrast, no striking nuclear accumulation of *OHO31* could be noticed at prophase of mitoses occurring during larval development (data not shown). The apparent low nuclear level of *OHO31* during later development may reflect the balance between the availability of *OHO31* and/or its rate of decay. A comparatively long prophase in imaginal tissues relative to the syncytial blastoderm may prevent any detectable nuclear accumulation of *OHO31*.

Although inactivation of the *oho31* gene causes growth inhibition in the ovaries and the developing wing imaginal discs, as revealed by mitotic recombination experiments (data not shown; Garcia-Bellido, A., and F. Cifuentes, personal communication), the absence of the same gene product in the hematopoietic organs and in the genital disc causes extensive cell proliferation and tumor formation. Thus, the absence of *OHO31* protein exerts opposite effects at the cellular level, causing either cell proliferation or arrest of cell growth. This difference may depend on the pattern of tissue differentiation. If the primary role of *OHO31* is to act as a cytosolic factor in nuclear transport, then we would predict that the absence of this protein would alter the cell cycle, but not necessarily prevent its completion, since alternative pathways may be used for nuclear protein import. Consequently, the duration of the cell cycle would be prolonged, and its extension may either delay or block terminal differentiation. For numerous cell types, a delay in the progression of differentiation would lead to growth arrest or be lethal, whereas for some other tissues, such as the hematopoietic organs, alteration in the progression of the cell cycle would cause continuous proliferation. Interestingly, we observe that, in aged tumors, the hemocytes become morphologically differentiated and have therefore lost their malignancy.

The authors thank Brigitte Heckmann, Dorothee Albrecht, Andrea Schrödel, and Gabriele Robinson for excellent technical assistance and Karin Helm for secretarial help.

This work was supported by grants to B. M. Mechler from the Deustche Forschungsgemeinschaft (436 UNG113/81/0), the Bundesministerium für Forschung und Technologie (Klinisch-Biochemischer Forschungswerbung), Fonds der chemischer Industrie, and the Commission of the European Union (contracts ERBSCI-CT92-0768, BMH1-94, 1572,

and ERBCIPACT922026-1194#1195) and by grants to I. Kiss from the National Scientific Research Foundation of Hungary (OTKA 924) and the Bástyai-Holzer Foundation. The *oho31* nucleotide data appears in the GenBank/EMBL/DDBJ under the accession number X85752.

Received for publication 25 November 1994 and in revised form 21 February 1995.

Note added in proof: Using a different approach P. Kussel and M. Frasch (Mount Sinai School of Medicine, New York) have independently isolated a sequence corresponding to *oho31* and encoding a protein designated as *Pendulin* (Kussel and Frasch. 1995. *J. Cell Biol.* 129:1491–1507).

References

Becker, H. J. 1959. Die puffs der Speicheldrüsenchromosomen von *Drosophila melanogaster*. I. Beobachtungen zum Verhalten des Puffmusters im Normalstamm und bei zwei Mutanten, *giant* and *lethal-giant-larvae*. *Chromosoma.* 10:654–678.

Belanger, K. D., M. A. Kenna, S. Wei, and L. I. Davis. 1994. Genetic and physical interactions beteen Srp1p and nuclear pore complex proteins Nup1p and Nup2p. *J. Cell Biol.* 126:619–630.

Bier, E., H. Vassin, S. Shepherd, K. Lee, K. McGall, S. Barbel, L. Ackerman, R. Caretto, T. Uemura, E. Grell, et al. 1989. Searching for pattern and mutation in the *Drosophila* genome with a P-lacZ vector. *Genes Dev.* 3:1273–1287.

Boedigheimer, M., and A. Laughon. 1993. *expanded*: a gene involved in the control of cell proliferation in imaginal discs. *Development.* 118:1291–1301.

Cavener, D. R. 1987. Comparison of the consensus sequence flanking translational start sites in *Drosophila* and vertebrates. *Nucleic Acids Res.* 15:1353–1361.

Chen, M. S., R. A. Obar, C. C. Schroeder, T. W. Austin, C. A. Poodry, S. C. Wadsworth, and R. B. Vallee. 1991. Multiple forms of dynamin are encoded by *shibire*, a *Drosophila* gene involved in endocytosis. *Nature (Lond.).* 352: 583–586.

Cortes, P., Z-S. Ye, and D. Baltimore. 1994. RAG-1 interacts with the repeated amino acid motif of the human homologue to the yeast protein SRP1. *Proc. Natl. Acad. Sci. USA.* 91:7633–7637.

Cuomo, C. A., S. A. Kirch, J. Gyuris, R. Brent, and M. A. Oettinger. 1994. Rch1, a protein that specifically interacts with the RAG-1 recombination-activating protein. *Proc. Natl. Acad. Sci. USA.* 91:6156–6160.

Dalby B., and D. M. Glover. 1992. 3′ non-translated sequences in *Drosophila* cyclin B transcripts direct posterior pole accumulation late in oogenesis and peri-nuclear association in syncytial embryos. *Development.* 115:989–997.

Dingwall, C., J. Robbins, S. M. Dilworth, B. Roberts, and W. D. Richardson. 1988. The nucleoplasmin nuclear location sequence is larger and more complex than that of SV40 large T antigen. *J. Cell Biol.* 107:841–849.

Foe, V. E., G. M. Odell, and B. A. Edgar. 1993. Mitosis and morphogenesis in the *Drosophila* embryo: point and counterpoint. *In* The Development of *Drosophila melanogaster*. M. Bate and A. Martinez Arias, editors. Cold Spring Harbor Laboratory Press, Cold Spring Harbor, NY. 149–300.

Franke, W. W., M. D. Goldschmidt, R. Zimbelmann, H. M. Mueller, D. L. Schiller, and P. Cowin. 1989. Molecular cloning and amino acid sequence of human plakoglobin, the common junctional plaque protein. *Proc. Nat. Acad. Sci. USA.* 86:4027–4031.

Frasch, M., M. Paddy, and H. Saumweber. 1988. Developmental and mitotic behavior of two groups of nuclear envelope antigens of *Drosophila melanogaster*. *J. Cell Sci.* 90:247–263.

Fuchs, J. P., H. Giloh, C.-H. Kuo, H. Saumweber, and J. Sedat. 1983. Nuclear structure: determination of the fate of the nuclear envelope in *Drosophila* during mitosis using monoclonal antibodies. *J. Cell Sci.* 64:331–349.

Gateff, E. 1978. Malignant neoplasms of genetic origin in *Drosophila melanogaster*. *Science (Wash. DC).* 200:1448–1459.

Gateff, E., and B. M. Mechler. 1989. Tumor suppressor genes of *Drosophila melanogaster*. *CRC Crit. Rev. Oncog.* 1:221–245.

Gateff, E., and H. A. Schneiderman. 1969. Neoplasms in mutant and cultured wild-type tissues of *Drosophila*. *Natl. Cancer Inst. Monogr.* 31:365–397.

Gateff, E., and H. A. Schneiderman. 1974. Developmental capacities of benign and malignant neoplasms of *Drosophila*. *Wilhelm Roux Arch. Entwicklungsmech. Org.* 176:23–65.

Görlich, D., S. Prehn, R. A. Laskey, and E. Hartmann. 1994. Isolation of a protein essential for the first step of nuclear protein import. *Cell.* 79:767–778.

Groden, J., A. Thliveris, W. Samowitz, M. Carson, L. Gelbert, H. Albertsen, G. Joslyn, J. Stevens, L. Spirio, M. Robertson, et al. 1991. Identification and characterization of the familial adenomatous polyposis coli gene. *Cell.* 66: 589–600.

Harel, E., E. Zlotkin, S. Naidel-Epszteyn, N. Feinstein, P. A. Fisher, and Y. Gruenbaum. 1989. Persistence of major nuclear envelope antigens in an envelope-like structure during mitosis in *Drosophila melanogaster* embryos. *J. Cell Sci.* 94:463–470.

Henikoff, S. 1984. Unidirectional digestion with exonuclease III creates targeted breakpoints for DNA sequencing. *Gene.* 28:351–359.

Jacob, L., M. Opper, B. Metzroth, B. Phannavong, and B. M. Mechler. 1987. Structure of the *l(2)gl* gene of *Drosophila* and delimitation of its tumor suppressor domain. *Cell.* 50:215–225.

Kemler, R. 1993. From cadherins to catenins: cytoplasmic protein interactions and regulation of cell adhesion. *Trends Genet.* 9:317–321.

Kikuchi, A., K. Kaibuchi, Y. Hori, H. Nonaka, T. Sakoda, M. Kawamura, T. Mizuno, and Y. Takai. 1992. Molecular cloning of the human cDNA for a stimulatory GDP/GTP exchange protein for ci-ki- *ras* p21 and *smg* p21. *Oncogene.* 7:289–293.

Kinzler, K. W., M. C. Nilbert, L. Su, B. Vogelstein, T. M. Bryan, D. B. Levy, K. Smith, A. C. Preisinger, P. Hedge, D. McKechnie, et al. 1991. Identification of FAP locus genes from chromosome 5q21. *Science (Wash. DC).* 253:661–665.

Mahoney, P. A., U. Weber, P. Onofrechuck, H. Biessmann, P. J. Bryant, and C. S. Goodman. 1991. The *fat* tumor suppressor gene in *Drosophila* encodes a novel member of the cadherin gene family. *Cell.* 67:853–868.

McCrea, P. D., C. W. Turck, and B. Gumbiner. 1991. A homology of the armadillo protein in *Drosophila* (Plakoglobin) associated with E-Cadherin. *Science (Wash. DC).* 254:1359–1361.

Mechler, B. M. 1990. The fruitfly *Drosophila* and the fish *Xiphophorus* as model systems for cancer studies. *Cancer Surv.* 9:505–527.

Mechler, B. M. 1994. Genes in control of cell proliferation and tumorigenesis in *Drosophila*. *In* The Legacy of Cell Fusion. S.Gordon, editor. Oxford University Press, Oxford, UK. 183–198.

Mechler, B. M., and D. Strand. 1990. Tumor suppression in *Drosophila*. *In* Tumor Suppressor Genes. Immunological Series Vol. 51. G. Klein, editor. Marcell Dekker, Inc., New York. 123–144.

Mechler, B. M., W. McGinnis, and W. J. Gehring. 1985. Molecular cloning of *lethal(2)giant larvae*, a recessive oncogene of *Drosophila melanogaster*. *EMBO (Eur. Mol. Biol. Organ.) J.* 4:1551–1557.

Patel, N. H., and C. S. Goodman. 1992. Digoxygenin labelled single-stranded DNA probes for in situ hybridization. *In* Nonradiactive Labelling and Detection of Biomolecules. C. Kessler, editor. Springer Verlag, Berlin. 377–381.

Peifer, M., S. Berg, and A. B. Reynolds. 1994. A repeating amino acid motif shared by proteins with diverse cellular roles. *Cell.* 76:789–791.

Picard, D., and K. Yamamoto. 1987. Two signals mediate hormone-dependent nuclear localization of the glucocorticoid receptor. *EMBO (Eur. Mol. Biol. Organ.) J.* 6:3333–3340.

Picard, D., V. Kumar, P. Chambon, and K. Yamamoto. 1990. Signal transduction by steroid hormones: nuclear localization is differentially regulated in estrogen and glucocorticoid receptors. *Cell Regul.* 1:291–299.

Poole, S. J., L. M. Kauvar, B. Drees, and T. Kornberg. 1985. The *engrailed* locus of *Drosophila*: structural analysis of an embryonic transcript. *Cell.* 40:37–43.

Powers, M. A., and D. J. Forbes. 1994. Cytosolic factors in nuclear transport: what's importin? *Cell.* 79:931–934.

Reynolds, A. B., L. Herbert, J. L. Cleveland, S. T. Berg, and J. R. Gaut. 1992. p120, a novel substrate of protein tyrosine kinase receptors and of $p60^{v\text{-}src}$, is related to cadherin-binding b-catenin, plakoglobin and *armadillo*. *Oncogene.* 7:2439–2445.

Riggleman, B., E. Wieschaus, and P. Schedl. 1989. Molecular analysis of the *armadillo* locus: uniformly distributed transcripts and a protein with novel internal repeats are associated with a *Drosophila* segment polarity gene. *Genes Dev.* 3:96–113.

Rizki, M. T. M. 1978. The circulatory system and associated cells and tissues. *In* The Genetics and Biology of Drosophila. Vol. 2b. M. Ashburner and T. R. F. Wright, editors. Academic Press, London. 397–452.

Robbins, J., S. M. Dilworth, R. A. Laskey, and C. Dingwall. 1991. Two interdependent basic domains in nucleoplasmin nuclear targeting sequence: identification of a class of bipartite nuclear targeting sequence. *Cell.* 64:615–623.

Sambrook, J., E. F. Fritsch, and T. Maniatis. 1989. Molecular Cloning: A Laboratory Manual. 2nd edition. Cold Spring Harbor Laboratory Press, Cold Spring Harbor, NY.

Shrestha, R., and E. Gateff. 1982. Ultrastructure and cytochemistry of the cell types in the larval hematopoietic organs and hemolymph of *Drosophila melanogaster*. *Devel. Growth and Differ.* 24:65–82.

Smith, D. E., and P. A. Fisher. 1984. Identification, developmental regulation, and response to heat-shock of two antigenically related forms of a major nuclear envelope protein in *Drosophila* embryos: application of an improved method for affinity purification of antibodies using polypeptides immobilized on nitrocellulose blots. *J. Cell Sci.* 99:20–28.

Stafstrom, J. P., and L. A. Staehelin. 1984. Dynamics of the nuclear envelope and of nuclear pore complexes during mitosis in the *Drosophila* embryo. *Eur. J. Cell Biol.* 34:179–189.

Stewart, M. J., and R. Denell. 1993. Mutations in the *Drosophila* gene encoding ribosomal protein S6 cause tissue overgrowth. *Mol. Cell. Biol.* 13:2524–2535.

Strand, D., I. Raska, and B. M. Mechler. 1994*a*. The *Drosophila lethal(2)giant larvae* tumor suppressor protein is a component of the cytoskeleton. *J. Cell. Biol.* 127:1345–1360.

Strand, D., R. Jakobs, G. Merdes, B. Neumann, A. Kalmes, H. W. Heid, I. Husmann, and B. M. Mechler. 1994b. The *Drosophila lethal(2)giant larvae* tumor suppressor protein forms homo- oligomers and is associated with nonmuscle myosin II heavy chain. *J. Cell Biol.* 127:1361–1373.

Suter, B., and R. Steward. 1991. Requirement for phosphorylation of the *bicaudal-D* protein in *Drosophila* oocyte differentiation. *Cell.* 67:917–926.

Tautz, D., and C. Pfeifle. 1989. A nonradioactive *in situ* hybridization method for the localization of specific RNAs in *Drosophila* embryos reveals transla-

tional control of the segmentation gene *Hunchback*. *Chromosoma*. 98:81–85.

Török, I., K. Hartenstein, A. Kalmes, R. Schmitt, D. Strand, and B. M. Mechler. 1993*a*. The *l(2)gl* homologue of *Drosophila pseudoobscura* suppresses tumorigenicity in transgenic *Drosophila melanogaster*. *Oncogene*. 8:1537–1549.

Török, T., G. Tick, M. Alvarado, and I. Kiss. 1993*b*. *P-lacW* insertional mutagenesis on the second chromosome of *Drosophila melanogaster*: isolation of lethals with different overgrowth phenotypes. *Genetics*. 135:71–80.

van der Bliek, A. M., and E. M. Meyerowitz. 1991. Dynamin-like protein encoded by the *Drosophila shibire* gene associated with phosphorylation on assembly of adherens-type junctions. *EMBO (Eur. Mol. Biol. Organ.) J.* 11: 1733–1742.

Watson, K. L., and P. J. Bryant. 1993. *Drosophila* tumor suppressor genes and carcinogenesis. *In* Proceedings of the Brystol-Myers Squibb Symposium on Cancer Research, Fox Chase Cancer Center, Philadelphia. R. Comis and A. Knudson, Jr., eds. Raven Press, New York. 121–135.

Watson, K. L., T. K. Johson, and R. E. Denell. 1991. *Lethal(1)aberrant immune response* mutations leading to melanotic tumor formation in *Drosophila melanogaster*. *Dev. Genet.* 12:173–187.

Watson, K. L., D. K. Konrad, D. F. Woods, and P. J. Bryant. 1992. The *Drosophila* homolog of the human S6 ribosomal protein is required for tumor suppression in the hematopoietic system. *Proc. Natl. Acad. Sci. USA*. 89: 11302–11306.

Wharton, R. P., and G. Struhl. 1991. RNA regulatory elements mediate control of *Drosophila* body pattern by the posterior morphogen *nanos*. *Cell*. 67:955–967.

Woods, D. F., and P. J. Bryant. 1991. The *discs-large* tumor suppressor gene of *Drosophila* encodes a guanylate kinase homolog localized at septate junctions. *Cell*. 66:451–464.

Woods, D. F., and P. J. Bryant. 1993. ZO-1, DlgA and PDS-95/SAP90: homologous proteins in tight, septate and synaptic cell junctions. *Mech. Dev.* 44:85–89.

Yano, R., M. Oakes, M. Yamaghishi, J. A. Dodd, and M. Nomura. 1992. Cloning and characterization of *SRP1*, a suppressor of temperature-sensitive RNA polymerase I mutations, in *Saccharomyces cerevisiae*. *Mol. Cell. Biol.* 12:5640–5651.

Yano, R., M. L. Oakes, M. M. Tabb, and M. Nomura. 1994. Yeast Srp1p has homology to armadillo/plakoglobin/β-catenin and participates in apparently multiple nuclear functions including the maintenance of the nucleolar structure. *Proc. Natl. Acad. Sci. USA*. 91:6880–6884.